UNIVERSITY OF INSUBRIA

PhD PROGRAM IN EXPERIMENTAL AND TRANSLATIONAL MEDICINE

XXIX CYCLE

Study of the molecular mechanism(s) underlying the antitumoral and highly pleiotropic functions of the human RNASET2 protein, a phylogenetically conserved extracellular RNase.

Tutor: Prof. Roberto Taramelli
Co-tutor: Prof. Francesco Acquati

PhD candidate:
Edoardo Pedrini

TABLE OF CONTENTS

INTRODUCTION 1

The Biological bases of Cancer 1

Macrophages functions and polarization patterns 3

The role of macrophages in cancer 4

The role of the RNASET2 gene in cancer 5

AIMS OF THE PROJECT 8

MATERIALS AND METHODS 9

Reagents and media 9

Cloning of the human RNASET2 coding sequence in plasmid vectors 9

Transformation of P. pastoris and "methanol utilization" phenotype screening 9

Expression of RNASET2 in P. pastoris 10

Purification of RNASET2 from P. pastoris supernatants by IMAC 10

Gravity-flow affinity chromatography 10

FPLC purification. 10

Analysis of RNASET2 expression by immunoblotting from conditioned media 10

Zymographic analysis 11

Animals and treatments 11

Optical and electron microscopy 12

Immunohistochemistry 12

Protein extraction and Western blot analysis 13

Extracts from tissue. 13

Extracts from adherent/suspended cells 13

BS3 crosslinking 13

NHS resin 14

Functionalization 14

Purification 14

Cells lines 14

RNASET2 Knockdown in THP-1 Cells 15

Differentiation and polarization protocol of THP-1 cells 15

Quantitative real time PCR 15

RESULTS 16

Recombinant human RNASET2 protein purification 16

Analysis of the evolutionary conserved relationship between RNASET2 and immune cells 22
Attempts to identify a putative receptor for RNASET2 33
Development of an assay to study the role of RNASET2 in macrophages polarization 35
DISCUSSION 40
Concluding remarks 45
REFERENCES 48
PUBLICATIONS 57

INTRODUCTION

The Biological bases of Cancer

Cancer is basically a large group of disease that can affect different part of the body [Nokhandani, 2015]. This might seem a very generic definition but correctly depicts the current state of our largely incomplete knowledge of the biology of this disease, which in turn demystify the idea of "a cure for cancer" [Simon, 2013].
Indeed, to gain more information concerning the still elusive biological bases of cancers current efforts are focused in particular towards a systems biology approach. Indeed, among several “systems” approaches, “omics” technologies are reaching competitive prices and the mechanistic description of biological systems through these methodological tools is increasing rapidly. We are entering a research age characterized by digital devices able to collect "big (personal) data” which are likely to detect alterations in biological networks parameters that might eventually predict when an organ will become diseased or when a perturbation in a biological network could progress to a disease state. Therefore, the most promising way for a treatment or prevention of cancer (and many other conditions) will be personalized predictions and personalized treatments [https://www.systemsbiology.org/research/p4-medicine/]

Despite the complexity and heterogeneity of these class of diseases, there are features that commonly characterize all cancers (depending on the specific staging) and altogether are classically referred to as the hallmarks of cancer [Hanahan, 2000].

The most important trait of cancer cells is their ability to sustain uncontrolled proliferation. At the molecular level, one of the strategy used to achieve this feature is the overexpression of growth factors, either by cancer cells themselves or by the surrounding stroma [Bhowmick, 2004]. As an alternative, receptor signaling can be de-regulated by the overexpression of receptor proteins or by the constitutive activation of signaling pathways operating downstream of these receptors [Lemmon, 2010].

A second hallmark of tumor cells is their ability to evade programs that negatively regulate cell proliferation. Many of these programs depend on the action of tumor suppressor genes. The two prototypical anti-oncogenes encode the retinoblastoma (RB) and the TP53 proteins, which operate within the regulatory circuits that govern the decision of a cell to proliferate or, alternatively, activate senescence and apoptotic death programs [Sherr, 2002].

Another common feature of tumor cells is the ability to escape programmed cell death (apoptosis), which is a natural barrier to cancer development. Cancer cells have evolved several different strategies to circumvent apoptosis, the most common being loss of the critical damage sensor TP53 gene, but the same result may be achieved by either overexpressing anti-apoptotic regulators (Bcl-2, Bcl-xL) or downregulating pro-apoptotic factors (Bax, Bim, Puma) [Evan, 1998].

Cancer cells also require unlimited replicative potential in order to generate tumors. Normal cells are able to carry out only a limited number of divisions and then enter senescence. The immortalization of tumor cells is achieved through several mechanisms and among them there is the ability to maintain telomeric DNA at lengths sufficient to avoid triggering senescence or apoptosis; this is achieved by upregulating

expression of telomerase or, less frequently, by an alternative recombination-based telomere maintenance mechanism [Shay, 2000].

Moreover, like normal tissues, tumors require nutrient and oxygen supplies as well as the ability to eliminate metabolic wastes and carbon dioxide. Thus, during tumor progression an angiogenic switch is activated, causing normally quiescent vasculature to continually sprout new vessels that help sustaining tumor growth [Hanahan, 1996].

Tumor cells often acquire the ability to locally invade tissues and/or metastasize. Typically, alterations in cancer cell shape as well as in attachment to other cells and to the extracellular matrix occur in this context. The invasion-metastasis cascade seems to involve discrete steps: local invasion; intravasation into nearby blood and lymphatic vessels; transit through the lymphatic and hematogenous systems; extravasation, micrometastases formation and colonization with development of macroscopic tumors [Talmadge, 2010].

More recently, two other distinctive characteristics of cancer cells have been proposed as emerging hallmarks [Hanahan, 2011]. The first involves reprogramming of cellular energy metabolism in order to support continuous cell growth and proliferation. The second involves active evasion by cancer cells from attack and elimination by immune cells [Hanahan, 2011].

Cancer has been studied as a clonal disease for many decades [Nowell, 1976] and the first theory introduced to explain its onset was the somatic mutation theory (SMT). According to this theory, cancer is the product of the accumulation of genetic lesions progressively selecting for the fittest (generally faster growing) cell clones. In support of this theory, a lot of known carcinogenic chemicals were found to be mutagenic. Moreover, tumors are characterized by aberrant transcriptional profiles and gain/loss of function mutations, both involving key regulatory genes (oncogenes/oncosuppressor genes) [Hanahan, 2011].

Although genetic aberrations represent a common feature of late-stage cancers, it is still largely debated whether mutations are the leading cause or just represent a side effect of carcinogenesis. Indeed, considering the rate of naturally occurring mutations and the large number of genetic and epigenetic changes that could in principle initiate and promote tumor development, cancer should paradoxically be ranked as a relatively rare disease, and cancer resistance rather that cancer occurrence might be worth investigating [Klein, 2007].
The recent advent of new technologies allowed a better understanding of multicellular systems and the heterogeneous nature of tumors is now recognized. Thus, cancer is now commonly viewed and analyzed as an evolving ecosystem [Gatenby, 2014] where, just like in any ecosystem, cancer cells engage in heterotypic interactions with cells in their microenvironment and use the available resources to proliferate and survive [Egeblad, 2010].
Within this framework, generally referred as tissue organization field theory (TOFT), most of the cancer research is now performed in order to provide new therapeutic solutions.
According to TOFT carcinogenesis acts initially by disrupting the normal interactions that take place among cells which compose the stroma and parenchyma of an organ [Sonnenschein, 2000].
One of the most interesting postulate of this theory is the reversibility of the states [Clark, 1991]. According to this theory, the neoplastic state of a cell is due to aberrant interactions and can be reversed or contained by “fixing” the context (meaning the microenvironment) of the cell [Bissell, 2001].

The high heterogeneity within both the tumor mass and the stromal compartment is the main hindrance to understanding the mechanisms that govern the interactions between cancer cells and the microenvironment. Different cell types are known to be present in the tumor surroundings: fibroblasts (cancer-associated fibroblasts, CAFs), endothelial cells, pericytes, immune inflammatory cells (tumor-associated macrophages, TAMs) and progenitor cells of the tumor stroma. All of these cells could have either a promoting or an inhibitory activity on tumor growth, depending on the context defined by the signaling networks.
Within this framework, the detailed investigation of the molecular interplay between cancer cells and the tumor microenvironment is essential in order to understand cancer initiation and progression, as well as to provide firm biological bases for new therapeutic solutions in cancer treatment.

Macrophages functions and polarization patterns

The accumulation of leukocyte subpopulations is the hallmark of several pathological conditions [Balkwill, 2001]. As discussed before, tumors are heterogeneous cellular ecosystems, a prominent component of which is represented by non-tumoral stromal cells like fibroblasts, endothelial cells and leukocytes. Among the latter, macrophages are the major component [Mantovani, 2002].

Macrophages represent a heterogeneous population of innate myeloid cells. They are found in all tissues and present a high variability in term of transcriptional profiles. Like other immune cells, they are characterized by high plasticity and tend to change their expressional profile based on the stimuli received from the environment. [Mantovani, 2005]
Their main function is to respond to pathogens and modulate the adaptive immune response through antigen processing and presentation, but they are also involved in the induction and resolution of inflammation, as well as tissue repair [Mosser, 2008].

The cytokine interleukin (IL)-4 was found to induce different effects on macrophage gene expression compared with the induction triggered by interferon (IFN)-gamma and lipopolysaccharide (LPS). In contrast to the classical "activation" pathway (induced by bacterial infections) of macrophages by IFN-gamma [Nathan, 1983], the macrophage gene expression induced by IL-4 was described as “alternative activation” [Stein M et al. 1992].

A few years later, Mills et al. proposed a new classification of macrophages as either M1 or M2. This terminology originated from an observation of differential macrophage arginine metabolism in various mouse strains with T helper type 1 (Th1) (C57BL/6 mice) and T helper type 2 (Th2) (Balb/c mice) backgrounds. Th1 mice with T cells producing mostly IFN-gamma showed a macrophage activation pattern in which nitric oxide (NO) was generated from arginine, versus ornithine production from Th2 mice with T cells producing IL-4 and tumor growth factor (TGF)-β 1 [Mills, 2000]. This finding led to a consensus within the scientific community that M1 (classically activated) macrophages exhibit inflammatory functions, whereas M2 (alternatively activated) macrophages exhibit anti-inflammatory functions.

In summary, the M1 macrophage phenotype is characterized by the production of high levels of pro-inflammatory cytokines, an ability to mediate resistance to pathogens, strong microbicide properties, high production of reactive nitrogen and oxygen intermediates, promotion of Th1 responses and cancer suppression. In contrast, M2 macrophages are characterized by their involvement in parasite control, tissue remodeling, immune regulation, tumor promotion and efficient phagocytic activity.

More recently, other authors expanded the M1-M2 definitions to account for different activation scenarios. According to this revised view, different mediators can be used in order to produce "polarized macrophages" and the classical M1 (INF-gamma + LPS) and M2 (IL-4) states represent just two prototypic cases within a spectrum of possible activation profiles that cannot be easily binned into defined groups [Stout, 2004; Mantovani, 2005; Edwards, 2006; Biswas, 2010; Martinez, 2014].
In experimental research (especially for in vitro systems) such poorly defined classification criteria to describe the real scenario of macrophages polarization represent a clear limitation.
In general, given that diverse mediators may be used alone or in various combinations for the generation of polarized macrophage populations, the recommendation is to adopt a nomenclature linked to the activation standards, i.e., M (IL-4) and M (IFN-g + LPS) instead of M2 and M1. Such nomenclature avoids the uncertainty of the classical definition, where one laboratory might experimentally define activation differently than another, and allows new activation conditions to be compared and contrasted with prototypical examples [Murray, 2014].

The role of macrophages in cancer

Macrophages derived from monocyte precursors undergo specific differentiation depending on the local tissue environment. In particular, they respond to environmental cues such as damaged cells, activated lymphocytes, or microbial products, to differentiate into distinct functional phenotypes [Mantovani 2002].
The first evidence of leukocyte infiltration into malignant tissue suggested that cancers arise at regions of chronic inflammation. In the tumor microenvironment, the specific subset of leukocyte that are characterized as macrophages have been called tumor associated macrophages (TAMs).
TAMs derive from circulating monocytes and are recruited at the tumor site by a tumor-derived chemotactic factor CCL2/MCP-1 [Matsushima, 1999].
Evidence supporting a pivotal role of chemokines in the recruitment of monocytes in neoplastic tissues comes from the high correlation between their production and infiltration in murine and human tumors [Rollins, 1999].
The cytokine network expressed at the tumor site plays a central role in the orientation and differentiation of recruited mononuclear phagocytes, thus contributing to direct the local immune system away from anti-tumor functions [Mantovani, 2002]. This idea is supported by both pre-clinical and clinical observations [Mantovani, 2004] and clearly demonstrate an association between macrophage number/density and prognosis in a variety of murine and human malignancies.
The immunosuppressive cytokines IL-10 and transforming growth factor (TGF)-β are produced by both cancer cells and TAMs [Mantovani, 2002]. IL-10 promotes the differentiation of monocytes to mature macrophages, blocks their differentiation to dendritic cells (DC) [Allavena, 2000] and promotes the alternative pathway of macrophage activation inducing TAMs to express M2-related functions.
Altogether, the production of IL-10, TGFβ and prostaglandin E2 (PGE2) by cancer cells and TAMs [Mantovani, 2002] contributes to a general suppression of anti-tumor activities.
TAMs are poor producers of NO [Dinapoli, 1996] and, in contrast to M1 polarized macrophages, have been shown to be poor producers of reactive oxygen intermediates (ROIs) [Klimp, 2001].

Angiogenesis is another M2-associated function, which represents a key event in tumor growth and progression. In human cervical cancer it has been proposed that VEGF-C production by TAMs play a role in peri-tumoural lympho-angiogenesis and subsequent dissemination of cancer cells with formation of lymphatic metastasis [Schoppmann, 2002]. Additionally, TAMs participate to the pro-angiogenic process

by producing the angiogenic factor thymidine phosphorylase (TP), which promotes endothelial cell migration in vitro and whose levels of expression are associated with tumor neovascularization [Hotchkiss, 2003].

Finally, TAMs express molecules able to remodel the surrounding connective tissue, providing advantages to tumor cell proliferation and spreading. In lung cancer, TAM may favor tumor progression by contributing to stroma formation and angiogenesis through their release of platelet derived growth factor (PDGF), in conjunction with TGF-β1 production by cancer cells [Mantovani, 2002]. Macrophages can produce enzymes and inhibitors that regulate the digestion of the extracellular matrix, such as matrix-metalloproteases (MMPs), plasmin, urokinase-type plasminogen activator (uPA) and the uPA receptor. Direct evidence has been presented that MMP-9 derived from hematopoietic cells of host origin contributes to skin carcinogenesis [Coussens 2000].
In summary, under many aspects TAMs display a number of functions expressed by M2 macrophages, involved in tuning inflammatory responses and adaptive immunity, scavenge debris, promote angiogenesis, tissue remodeling and repair [Locati, 2002].

Although TAMs and their relationship with tumor cells have been extensively studied, several experiments have demonstrated that macrophages have the potential to kill tumor cells *in vitro* when appropriately stimulated.
Solid tumors establish physical/chemical barriers to prevent entry of immune cells in order to escape from immune surveillance, but TAMs (which represent a component of the stroma and are usually there to assist tumor progression) may be the target of a re-education from a tumor-supportive phenotype to a tumor-suppressive phenotype [Wang, 2017].
Recent studies which used cells or microspheres as biological vectors to deliver therapeutic molecules specifically to the neoplastic site made some significant effects. In a metastatic prostate cancer animal model, intratumoral injection of macrophages transduced with IL-12 recombinant adenovirus vector led to the reduction of primary prostate cancer growth and lung metastases [Satoh, 2003].
IL-12 is a key immunoregulatory cytokine, it is produced mainly by antigen-presenting cells and can regulate innate responses [Breading, 2006]. IL-12 determines the type of adaptive immune responses during infection triggering CD4-T cells to differentiate into Th1 cells which in turn stimulate the classical activation of local macrophages [Hamza, 2010].

To conclude, a high M1/M2 ratio has been reported to be associated with an improved survival in solid tumors [Pollard, 2008]. Nevertheless, bacterial stimuli and Th1 cytokines inducing M1 type polarization are usually not present at the tumor site. Here, in contrast, differentiating macrophages are likely to encounter factors that most frequently polarize them toward M2 type macrophages.
Therefore, the manipulation of the tumor microenvironment aimed to the re-education of TAMs may have promising applications in the field of tumor immune therapy.

The role of the RNASET2 gene in cancer

Loss of heterozygosity (LoH) studies have long been used as powerful tools to obtain molecular evidence for the subchromosomal localization of putative human tumor suppressor genes (TSGs).
In this context, LoH studies carried out in the last decades on ovarian tumors and ovarian cancer cell lines have consistently reported chromosomal loss on human chromosomes 1, 6, 9, 10 and 11 for this cancer type [Nakayama, 2007; Tapper, 1997; Suehiro, 2000]. Particularly, three different *consensus* regions of LoH in human chromosome 6 were identified: 6q21-23.3 [Orphanos, 1995], 6q25.1-25.2 [Colitti, 1998]

and 6q.26-27 [Saito, 1992; Tibiletti, 1996]. The human *RNASET2* gene maps within the latter chromosomal region. *RNASET2* is a 27 kb single-copy gene composed by nine exons and eight introns [Tibiletti, 1998] and coding for the unique human member of the extracellular Rh/T2/S ribonuclease gene family.
Ribonucleases represent a wide family of enzymes able to process or degrade ribonucleic acids. Historically, investigations have focused on ribonucleases belonging to the RNase A family members, which are limited to vertebrate species [D'Alessio; 1997]. However, a growing interest has been recently focused on the highly conserved Rh/T2/S RNAse family [McClure, 1990], due to their very high evolutionary conservation and their involvement in several key cellular and biological processes, such as nutritional stress response [Liang, 2002], neural development [Henneke, 2009], modulation of the immune response [Steinfelder, 2009], cell death [Thompson, 2009], cancer growth control [Acquati, 2011, 2013] and stress response [Lualdi, 2015], to name a few.

The human RNASET2 protein is composed by 256 amino acids and its primary sequence reveals the presence of three distinct protein segments: a signal peptide for secretion at the N-terminus (aa. 1-24), a central core that undergoes N-glycosylation and carries the two conserved active-site segments (CASI and CASII) responsible for the catalytic activity of the protein and a C-terminal de-structured portion [Campomenosi, 2006].
The RNASET2 protein is commonly detected in three different intracellular isoforms: a full-length 36 kDa form, which is secreted in the extracellular space, and two 31 and 27 kDa isoforms, which originate from proteolytic cleavage at the C-terminus of the full-length protein. By sub-cellular fractionation assays, both 31 and the 27 kDa isoforms were detected in the lysosomal fraction. This observation is consistent with the hypothesis of a functional role of RNASET2 as an acid ribonuclease in the acid lysosomal compartment [Campomenosi, 2006]. Moreover, localization of RNASET2 protein in processing bodies (P-bodies) has also been reporter under stress condition [Vidalino, 2012]. As for the ribonuclease activity of RNASET2 protein, it shows a base preference for poly-A and Poly-U synthetic polynucleotides, with respect to Poly-G and Poly-C, at pH 5.0 [Campomenosi, 2006].

Because of the chromosomal location of the human RNASET2 gene in a region frequently rearranged in tumors, its putative tumor suppressive role has been thoroughly investigated in recent years.
Using the ovarian carcinoma as an experimental model, no mutations were found in the coding sequence of the RNASET2 gene in human primary ovarian tumors and tumor cell lines [Acquati, 2001]. However, RNASET2 down-regulation at the mRNA level was reported in both primary ovarian tumors and ovarian tumor cell lines, with respect to normal tissue/cells. In order to understand the molecular bases of the lower RNASET2 expression levels in tumors, a promoter methylation analysis was performed, but no significant differences in promoter methylation were reported between tumor and normal samples, suggesting that other epigenetic mechanisms could be responsible for RNASET2 hypoexpression in tumors [Acquati, 2001].

However, a marked RNASET2-mediated tumor suppression *in vivo* has been demonstrated using both ovarian carcinoma and malignant melanoma as experimental models. Indeed, RNASET2-overexpressing tumor clones turned out to be strongly suppressed in their tumorigenic and metastatic potential after injection in immunodeficient mice [Acquati, 2001].
On the basis of this evidence, RNASET2 was defined as a class II tumor suppressor gene, being hypoexpressed in tumors despite the absence of structural alterations in the sequence of the gene.

To address the role of the catalytic activity of RNASET2 protein in the observed *in vivo* tumor suppression, Hey3Met2 ovarian tumor clones overexpressing a catalytically inactive form of the protein were

generated. The catalytically-dead form of the protein was obtained by replacement of the two key Histidine residues in CAS sites (H65 and H118) with two Phenylalanine residues.
Strikingly, RNASET2-mediated tumor suppression turned out to be independent of the ribonuclease activity of the protein. Indeed, using xenograft models in nude mice, RNASET2 H65/118F-overexpressing Hey3Met2 clones resulted to be suppressed in their tumorigenicity as well as their RNASET2 wild type-overexpressing counterpart [Acquati, 2005].

Moreover, a close histological examination of xenograft tumors sections revealed a consistent infiltrate of host cells in tumors derived from RNASET2-overexpressing Hey3Met2 clones. Analysis with specific cell-surface markers demonstrated that the infiltrate was mainly due to cells belonging to the monocyte-macrophage cell lineage [Acquati, 2011]. In the same direction, inoculation of nude mice with human ovarian cancer-derived cells with high endogenous RNASET2 expression levels (OVCAR3) led to the development of small, growth-suppressed tumors, characterized by a strong infiltrate of host-derived innate immunity cells, which have been identified as M1 polarized macrophages. By contrast, RNASET2-silenced OVCAR3 cells developed large, fast-growing tumors with no sign of macrophage infiltration [Acquati, 2013].

To further investigate the role of the monocyte-macrophage cell population in the RNASET2-mediated tumor suppression, a new experimental *in vivo* model was exploited, in which the monocyte-macrophage lineage was depleted by clodronate treatment in RAG-γ chain mice. In this model, RNASET2-mediated tumor suppression activity was drastically impaired in clodronate-treated mice when compared to untreated control mice [Acquati, 2011].
Finally, the involvement of RNASET2 in the recruitment of cells belonging to the monocyte linage has been also assessed *in vitro*; by these assays, recombinant RNASET2 protein displayed a marked chemotactic activity *in vitro,* possibly dependent from a subfamily of GPCR associated with inhibitory G protein [Acquati, 2013].
Taken together, these data suggest that the tumor microenvironment and particularly the monocyte-macrophage cell population seems to play a crucial role in RNASET2-mediated tumor suppression *in vivo*.

AIMS OF THE PROJECT

The *RNASET2* gene encodes for the only human secreted acid ribonuclease of the T2 family. This gene maps to human chromosome 6q27, a region that is consistently found rearranged in many solid and hematological tumors [Acquati, 2005]. Experimental data have demonstrated the role of RNASET2 as a tumor suppressor gene which is endowed with several functions including chemotactic and possibly activating activity toward the monocyte/macrophage population [Acquati, 2011].
In a mouse xenograft model, we have recently reported that inoculation of human ovarian cancer-derived cells forced to overexpress RNASET2 led to the development of small, growth-suppressed tumors, characterized by a strong infiltrate of host-derived innate immunity cells, which have been identified as M1 polarized macrophages. By contrast, control cells expressing RNASET2 at lower level (or silenced by RNA interference), developed large, fast-growing tumors with no sign of macrophage infiltration.
Further investigations proved that recombinant RNASET2 (produced with both baculovirus and *Pichia pastoris* expression system) displayed a marked chemotactic activity *in vitro,* possibly dependent from a subfamily of GPCR associated with inhibitory G protein [Acquati, 2013].
Taken together, these results led us to suggest that the observed *in vivo* tumor suppression is a non-cell-autonomous effect based on RNASET2-mediated recruitment of macrophages into the tumor mass.
Based on these experimental data, we decided to further investigate the functional implications of the interaction between RNASET2 and the monocyte-macrophages, following different approaches as outlined below:

- Since a considerable amount of protein is required to perform functional studies, we improved our heterologous expression systems for production and purification of endotoxin-free recombinant RNASET2.
- The functional interaction of RNASET2 with innate immune cells has been investigate in an independent, cost-effective in *vivo* system represented by the leech *Hirudo verbana*.
- Based on our previous *in vitro* data (chemotaxis and internalization assays) we hypothesized the occurrence of a cellular system able to “sense” extracellular RNASET2 protein. The existence of a putative cell surface receptor for RNASET2 was therefore investigated.
- Our previous *in vivo* data showed that the stromal cell infiltrate in RNASET2-expressing tumors was represented by M1-polarized macrophages. The role of recombinant RNASET2 in macrophage differentiation and polarization was therefore investigated.

MATERIALS AND METHODS

Reagents and media

The EasySelect™ Pichia Expression Kit was available from Invitrogen (Thermo Fischer Scientific, Waltham, MA, USA). Phusion® High-Fidelity DNA Polymerase and restriction/modification enzymes were from New England Biolabs (NEB, Ipswich, MA, USA). Zeocin was purchased from InvivoGen (InvivoGen, Toulose, France). Yeast Nitrogen Base from Difco BD (Becton Dickinson and Company, Franklin Lakes, NJ, USA).
Bradford reagent and Polyprep columns were from Bio-Rad (Bio-Rad laboratories, Hercules, CA, USA). Ultrafree centrifugal concentrators (5 kDa MWCO) were from Merck Millipore (EMD Millipore, Billerica, MA, USA), VivaFlow 50 cross flow cassettes (10 kDa MWCO) from Sartorius (Sartorius AG, Gottingen, Germany), Slide-A-Lyzer dialysis cassettes (10 kDa MWCO) from Thermo Scientific (Thermo Fischer Scientific, Waltham, MA, USA). Ni-NTA resins were obtained from Qiagen (Qiagen N.V., Venlo, Netherlands); HisTrap HP (1 ml), HiTrap Q HP (1 ml) and Superdex 75 10/300 GL columns were from GE Healthcare (General Electric Co., Fairfield, CT, USA). NuPAGE Bis-Tris precast gels were from Life Technologies (Thermo Fischer Scientific, Waltham, MA, USA), nitrocellulose and PVDF membranes were from GE Healthcare (General Electric Co., Fairfield, CT, USA). SuperSignal® West Dura Extended Duration Chemiluminescent Substrate was available from Thermo Scientific (Thermo Fischer Scientific, Waltham, MA, USA). All other reagents were from Sigma-Aldrich (Sigma-Aldrich Corporation, St. Louis, MO, USA), unless otherwise stated.

Cloning of the human RNASET2 coding sequence in plasmid vectors

Cloning of the wild-type (wtRNASET2) RNASET2 coding sequences, fused at the 3'-end to sequences coding for both HA (hemagglutinin) and 6xHistidine tags into the pPICZαA expression vector, have been described previously (pPICZαA-wtRNASET2 and pPICZαA-RNASET2 H65/118F [Campomenosi, 2011]. In order to improve the efficiency of the purification steps we decided to clone the wild-type RNASET2 coding sequence with an additional 6xHis tag at the 5'-terminus (pPICZαA-wt2tag RNASET2). The pPICZαA-wtRNASET2 construct was used as a template for a PCR reaction with the following primer pair (5'-3'):
RNASET2 fw Eco6XHis 25aa: ACTGGAATTCCATCACCACCATCATCACGACAAGCGCCTGCGTGAC
3'AOX rev: GCAAATGGCATTCTGACATCC
The amplification product was digested with EcoRI and XhoI, gel purified and cloned into pPICZαA before transforming in the DH5α *E. coli* strain. Plasmid DNA was purified and, after sequencing (BMR, Padova, Italy), the empty vector and pPICZαA-wt2tag RNASET2 construct were used to transform X33 *P. pastoris* strain.

Transformation of P. pastoris and "methanol utilization" phenotype screening

RNASET2-coding construct or empty vector were linearized within the 3'AOX region with PmeI restriction enzyme and transformed into *P. pastoris* by the lithium chloride method [Gietz, 1995]. The methanol utilization plus (Mut+) X33 strain was transformed. Transformants were selected on Yeast Extract Peptone Dextrose (YPD) plates (1% yeast extract, 2% bactopeptone, 2% dextrose, 20 g/l bactoagar) containing 100 µg/ml Zeocin and confirmed by streaking on the same plates. Zeocin-resistant clones were picked and lysed by boiling at 100°C for 10 min. PCR reactions were performed on lysates according to manufacturer's instructions in order to discriminate integration of the empty vector from integration of RNASET2-containing constructs. Mut+ strain colonies positive for integration were also screened for the methanol utilization phenotype by streaking on MDH and MMH plates (Minimal Dextrose Histidine and Minimal

Methanol Histidine: 1,34% yeast nitrogen base, $4x10^{-5}$% biotin, 0.004% histidine, 15 g/l bactoagar and either 2% dextrose for MDH or 0.5% methanol for MMH plates).

Expression of RNASET2 in P. pastoris

Buffered complex glycerol or buffered complex methanol (BMGY/BMMY) (1% yeast extract, 2% bactopeptone, 1,34% yeast nitrogen base, $4x10^{-5}$% biotin and either 1% glycerol or 0.5% methanol) media were used to grow cells and analyze the expression of RNASET2. Briefly, selected clones were plated and grown for 3 days at 28°C. One colony was picked and inoculated into 50 ml of BMGY medium. Cultures were grown at 28°C overnight until they reached an Optical Density at 600 nm (OD_{600}) between 2 and 6. They were then centrifuged and the cell pellet was resuspended in BMMY at a starting OD_{600} of 1 for induction of protein expression. Fresh methanol (0.5% final concentration) was added to the culture each day, from time 0 to 7 days from the first induction.

Purification of RNASET2 from P. pastoris supernatants by IMAC

Cell cultures were processed after 7 days from induction and the best producer clone was selected to express the protein for subsequent purification. After pelleting the cells at 2500 g in a swinging bucket rotor, the supernatant was filtered (0.45 µm) and processed.

Gravity-flow affinity chromatography. Conditioned media were concentrated (10 kDa cut-off) and then incubated with the Ni-NTA Agarose matrix, in the presence of 10 mM imidazole (Qiagen). Post-binding the mixtures (medium/resin) were poured into columns. The flow-through, wash (50 mM imidazole) and eluate fractions (250 mM imidazole) were collected and analyzed by SDS-PAGE (silver staining) and immunoblotting.

FPLC purification. Conditioned media (500 ml to 1l volumes) from *P. pastoris* cultures expressing RNASET2 protein were concentrated by ultrafiltration on VivaFlow 50 cross-flow cassettes (10 kDa MWCO) to final volumes of 20 to 50 ml. The concentrated solutions were extensively dialyzed against PBS (20 mM Na-Phosphate, 150 mM NaCl, pH 7.50) using Slide-A-Lyzer dialysis cassettes (10 kDa MWCO) and adjusted to 500 mM NaCl and 10 mM Imidazole final concentrations prior to loading onto a HisTrap HP (1 ml) column equilibrated with PBS containing 500 mM NaCl and 10mM Imidazole (equilibration buffer). Retained proteins were eluted at 1 ml/min using a step gradient of Imidazole in equilibration buffer. Eluates from the HisTrap column were further purified by negative-mode anion exchange chromatography (i.e., RNASET2 proteins passed through the stationary phase and contaminants were retained on it). To this end, protein solutions from HisTrap were made 100 mM NaCl by dilution with buffer A (20 mM Tris-Cl, 100 mM NaCl, pH 7.50), then loaded onto a HiTrap Q XL (1 ml) column equilibrated with buffer A at 1 ml/min and eluted with a step gradient of buffer B (20 mM Tris-Cl, 1M NaCl, pH 7.50). Where described, aliquots of both manually (i.e., from Ni-NTA resin) and FPLC (i.e., from either HisTrap or HiTrap Q columns) purified proteins were chromatographed on a Superdex 75 10/300 GL gel filtration column, using PBS as eluent at 0.5 ml/min. In all cases, chromatography columns were mounted onto ad operated by an ÄKTA Purifier FPLC system, and protein elution was monitored as UV absorbance at 280 nm.

Analysis of RNASET2 expression by immunoblotting from conditioned media

Aliquots of conditioned media from RNASET2-expressing *P. pastoris* cultures as well as relevant fractions from chromatography were separated on either 4-12% and 10% Bis-Tris or 13% Tris-Glycine gels. Proteins were either revealed by Silver Staining (Sigma-Aldrich) or transferred onto PVDF/nitrocellulose membranes. These were saturated with either PBS or Tris-buffered saline (TBS) containing 5% (w/v) non-

fat dry milk and RNASET2 proteins were revealed with selected primary antibodies (i.e., either rabbit anti-RNASET2 polyclonal antibody or mouse anti-His tag monoclonal antibody) followed by the appropriate horseradish peroxidase-conjugated anti-mouse or -rabbit IgG secondary antibody. Membranes were incubated with SuperSignal® West Dura Extended Duration Chemiluminescent Substrate and chemiluminescence recorded on a Chemidoc® MP system (Bio-Rad) or X-Ray films (Thermo Scientific).

Zymographic analysis

To verify the acquisition of the proper folding, we assess the catalytic activity of recombinant RNASET2 protein purified from *P. pastoris* supernatants performing a zymographic analysis. Polyacrylamide gels were prepared with the addition of total RNA from Torula yeast in resolving (2 mg/ml) and stacking (0.3 mg/ml) gel solutions. Proteins were diluted in non-reducing sample buffer (125 mM Tris-HCl pH 6.8, 2% SDS, 10% glycerol, 0,02% bromophenol blue) and loaded without boiling. After electrophoresis, SDS was removed with 25% isopropanol dissolved in wash solution (10 mM Tris-HCl, pH 7.4), then gels were washed extensively and incubated at 51°C in freshly prepared activity buffer (100 mM KCl, 100 mM Sodium acetate, pH 5.0). Enzymatic activity was detected by bleaching of the toluidine blue staining. After image acquisition, gels were completely destained and processed for immunoblotting.

Animals and treatments

Leeches H. medicinalis (Annelida, Hirudinea, from Ricarimpex, Eysines, France) measuring 10 cm were kept in water at 20 °C in aerated tanks and fed weekly with calf blood. For each experimental group, treatment (PBS, LPS, recombinant protein or matrigel injection) was performed at the level of the 80th superficial metamere on leeches anaesthetized with a 10 % ethanol solution. Treated and control untreated animals were anesthetized and then dissected to remove body wall tissues or matrigel pellets at specific time points (T24h, T7days). Animals were randomly split into eight separate experimental groups (five individuals for each time point) and submitted to various protocols and treatments.

Group 1: control animals (uninjected)

Group 2: control animals injected with 100 µl sterilized PBS (138 mM NaCl, 2.7 mM KCl, 4.3 mM Na2HPO4, 1.5 mM KH2PO4, pH 7.4) and analyzed at T24 h and T7 days.

Group 3: animals injected with 100 µl sterilized PBS containing 20ng of recombinant hRNASET2 protein and analyzed at T24 h and T7 days to functionally characterize cells migrating under the influence of this factor. The best concentration of hRNASET2 required to induce significant cell migration was determined based on previous works [Grimaldi, 2011];

Group 4: animals injected with 100 µl of sterilized PBS containing 50 ng of recombinant hRNASET2 previously incubated for 1h at room temperature with 1µg of anti-hRNASET2 specific polyclonal antibody [Campomenosi, 2011] to perform antibody-mediated neutralization experiments, analyzed at T24 h and T7 days.

Group 5: animals injected with 100 µl of PBS containing 100 ng/ml LPS obtained from E. coli (Serotype 0111: B4, Sigma, St. Louis, MO, USA) in order to evaluate the expression of RNASET2 in cells involved in innate immune response, analyzed at T24h.

Group 6: control animals injected with 300 µl of liquid matrigel MG (an extract of the murine Engelbreth–Holm–Swarm (EHS) tumor produced as previously described) [Kleinman, 1986], analyzed at T7 days.

Group 7: animals injected with 300 µl of liquid MG supplemented with 50ng of hRNASET2, were used to selectively isolate the cells migrating under the influence of RNASET2 and were analyzed at T7 days.

Group 8: animals injected with 300 µl of liquid MG supplemented with 50 ng of hRNASET2 and 1µg of the polyclonal antibody RNASET2, used for antibody-mediated neutralization experiments and analyzed at T7 days.

Optical and electron microscopy

Leech tissues, dissected from the area of the injection, were fixed for 2 h in 0.1 M cacodylate buffer at pH 7.4, containing 2 % glutaraldehyde. Specimens were then washed in the same buffer and postfixed for 1 h with 1 % osmium tetroxide in cacodylate buffer, pH 7.4. After standard serial ethanol dehydration, specimens were embedded in an EponAraldite 812 mixture. Sections were obtained with a Reichert Ultracut S ultratome (Leica, Wien, Austria). Semi-thin sections were stained by crystal violet and basic fuchsine and subsequently observed under a light microscope (Nikon Eclipse Ni, Nikon, Tokyo, Japan). Data were recorded with a DS-5 M-L1 digital camera system (Nikon). Ultrathin sections were placed on copper grids, stained by uranyl acetate and lead citrate and observed with a Jeol 1010 EX electron microscope (Jeol, Tokyo, Japan).

Immunohistochemistry

Samples (leech tissues and matrigel pellets), were embedded in Polyfreeze tissue freezing medium (OCT) (Polysciences, Eppelheim, Germany) and immediately frozen in liquid nitrogen. Cryosections, obtained with a Leica CM 1850 cryotome. For a morphological view serial cryosections were stained by crystal violet and basic fuchsine. For immunofluorescence staining, sections, rehydrated with PBS for 5 min, were pre-incubated for 30 min with PBS containing 2 % bovine serum albumin (BSA) before incubation (1 h at 37 °C) with the following primary polyclonal antibody diluted in blocking solution: rabbit anti-human anti-RNASET2 [Campomenosi , 2011], diluted 1: 200; rabbit anti-human CD68 (Santa Cruz Biotechnology, Calif., USA), which reacts, as previously demonstrated, with leech macrophage-like cells [de Eguileor, 2003], diluted 1:100; rabbit anti-H.medicinalis HmAnti-AIF-1 (specific marker for macrophages leech [Drago, 2014] and kindly donated by Prof. Jacopo Vizioli, University of Lille 1, France, diluted 1: 1000. The washed specimens were incubated for 1h at room temperature with the appropriate secondary antibodies (Abcam, Cambridge, UK), diluted 1:200, goat anti-rabbit Cy5-conjugated (excitation filter 650 nm, emission filter 672 nm) or goat anti-rabbit fluorescein isothiocyanate (FITC)-conjugated (excitation 493 nm, emission 518 nm). Double labelling experiments were performed as previously described [Grimaldi, 2009]

to detect RNASET2 /HmAIF-1 or RNASET2 / CD68, RNASET2 was applied first and then sections were incubated with the secondary antibody, goat anti-rabbit (Cy5)-conjugated. According to Würden and Homberg [Würden, 1993], to inhibit binding of the primary antiserum of the second staining cycle to the goat anti-rabbit IgGs that were applied in the first sequence, the sections were incubated with rabbit IgG (Jackson ImmunoResearch) at 1:25 for 2 h. After washing the samples were incubated with the antibody anti HmAIF-1 or anti CD68. Subsequently, the sections were treated with the secondary (FITC)-conjugated goat antirabbit antibody. According to Schnell and colleagues [Schnell, 1999], after immunocytochemistry, the sections were treated with 1 mM $CuSO_4$ in 50 nM ammonium acetate buffer (pH 5.0) for 15 min and then washed in distilled water and PBS. Application of $CuSO_4$ for 10 minutes after immunohistochemistry substantially reduced tissue autofluorescence while preserving the specific fluorochrome signal. In all controls experiments primary antibodies were omitted and sections were incubated only with the secondary antibodies. Nuclei were stained by incubating for 15 min with 49,6-Diamidino-2-Phenylindole (DAPI, 0.1 mg/ml in PBS, excitation 340 nm, emission 488 nm). The slides were mounted in Citifluor (Citifluor, London, UK) with coverslips and examined with a Nikon fluorescence microscope or with a confocal laser microscope (Leica TCS SP5). Images were combined with Adobe Photoshop (Adobe Systems Incorporated, San Jose, CA, USA).

Protein extraction and Western blot analysis

Extracts from tissue. H. medicinalis tissues extracted from the unstimulated body wall or from injected areas were immediately frozen in liquid nitrogen and then homogenized with a mortar. For SDS-PAGE, leech homogenates were suspended (10 µl per mg of tissue), in RIPA buffer (150 mM NaCl, 1% NP-40, 0,5% Sodium deoxycholate, 0,1% SDS, 50 mM Tris-HCl pH 8.0) in the presence of a protease inhibitor cocktail (Sigma, Milan, Italy). The particulate material was removed by centrifugation at 13,000 rpm for 10 min at 4 °C in a refrigerated Eppendorf Minispin microcentrifuge (Eppendorf, Hamburg, Germany). Supernatants were collected, denatured at 95 °C for 5' min and loaded on 10 % acrylamide for SDS-PAGE analyses. Immunoblot analysis was performed using standard procedures and detected with a chemiluminescent substrate (Super-signal *West Dura* extended duration kit, Thermo Scientific).

Extracts from adherent/suspended cells. Adherent cells were mechanically scraped in PBS + 5mM EDTA and resuspended in lysis buffer (0.5% Igepal, 0.5% Triton X-100 in PBS + 5mM EDTA) supplemented with protease inhibitors cocktail. Suspended cells were collected, washed and resuspended in lysis buffer.
Samples were kept 45' in a rotor stator at 4 °C; the particulate material was removed by centrifugation at 13,000 rpm for 10 min at 4 °C and supernatants were collected and quantified with Bradford reagent (bovine serum albumin was used as standard).
For the SDS-PAGE analysis, 30-70 µg of intracellular lysate were denatured at 95°C for 5' in RIPA buffer and loaded on 10 % acrylamide for SDS-PAGE analyses. Immunoblot analysis was performed using standard procedures and detected with a chemiluminescent substrate (Super-signal *West Dura* extended duration kit, Thermo Scientific).

- anti-RNASET2 (Davids Biotechnologie GmbH, Regensburg, Germany). 1:500 in 5% PBS-milk for 60'. HRP anti-rabbit IgG (Jackson ImmunoResearch Laboratories, West Grove, USA) 1:5000 in 2% PBS-T-milk + 0.1% SDS for 45'.
- anti-HmAIF-1 1:5000 in 5 % TBS-milk for 60'. HRP anti-rabbit IgG 1:5000 in 5% TBS-milk for 45'.
- anti-tubulin (Proteintech, Chicago, USA) 1:1500 in 5% PBS-milk for 60'. HRP anti-rabbit IgG 1:5000 in 2% PBS-T-milk + 0.1% SDS for 45'.
- anti-human GAPDH (Proteintech, Chicago, USA) 1:2000 in 5% PBS-milk for 60'. HRP anti-rabbit IgG 1:5000 in 2% PBS-T-milk + 0.1% SDS for 45'.

BS3 crosslinking

Suspend cells at ~25 × 10^6 cells/mL in PBS (pH 8.0) and wash cells three times with ice-cold PBS (pH 8.0) to remove amine-containing culture media and proteins from the cells.
Add ligands to the cells and incubate for 1 hour at 4°C. Add the BS3 solution to a final concentration of 5mM.
Incubate the reaction mixture for 30 minutes at room temperature. Add the Quench Solution 91M Tris-HCl, pH 7.5) to a final concentration of 20mM Tris, incubate for 15 minutes at room temperature and proceed with protein extract.

NHS resin

Functionalization. Prepare protein or peptide solution in Coupling Buffer (0.1M sodium phosphate, 0.15M NaCl, pH 7.2) for direct addition to the desired amount of dry resin. Place an appropriate amount of dry NHS-Activated Agarose resin to an empty spin column and add the protein or peptide sample directly to the dry resin (use at least twice the sample volume to swell volume. The resin swell volume is 6-7.5mL of wet resin per gram of dry resin. For the 33mg spin column, use 400µL of sample; for the 330mg spin column, use 4mL of sample). Replace the top cap on the column and mix the reaction end-over-end for 1 hour (approximately 80% of the reaction occurs in the first 30 minutes. The reaction may be extended to 2 hours at room temperature or overnight at 4ºC). Remove top and bottom caps and place the column in a collection tube. Centrifuge at 1000 × g for 1 minute and save the flow-through. Add Coupling/Wash Buffer (twice the volume of the resin) to the column, centrifuge at 1000 × g for 1 minute and save the wash fraction. Repeat this step once (the saved flow-through and washes can be used to determine the coupling efficiency by comparing the protein concentrations of these non-bound fractions to the starting sample). Add Quenching Buffer (1M Tris, pH 7.4, twice the volume of the resin) to the column and replace the bottom cap. Replace the top cap and mix end-over-end for 15-20 minutes at room temperature. Remove the top cap and then the bottom cap. Place the column in a new collection tube, centrifuge at 1000 × g for 1 minute and discard the flow-through. Wash column with Coupling/Wash Buffer. Monitor the final washes for the presence of protein by measuring absorbance at 280nm or by the Pierce 660nm Protein Assay. Either proceed directly with affinity purification or prepare column for storage. For storage, wash column with PBS containing 0.05% sodium azide or other preservative. Replace bottom cap when 0.5-1mL of buffer remains above the resin bed. Replace top cap and store column upright at 4°C.

Purification. Equilibrate the prepared affinity column to room temperature. Remove top and bottom caps and place column in a collection tube. Centrifuge the column at 1000 × g for 2 minutes to remove the storage solution. Equilibrate column by adding Binding Buffer (0.1M sodium phosphate, 0.15M NaCl, pH 7.2) and centrifuge at 1000 × g for 2 minutes. Discard buffer from collection tube. Repeat this step twice. Add sample to column and allow it to enter the resin bed. Replace top and bottom caps on the column. Incubate the column 2 hours at room temperature with end-over-end mixing. Remove top cap and bottom caps from column and place column in new collection tube. Centrifuge the column at 1000 × g for 2 minutes. Save the flow-through to analyze binding efficiency. Wash the column with of Binding/Wash Buffer. Centrifuge at 1000 × g for 2 minutes.

Elute the bound protein by applying Elution Buffer (0.2M glycine-HCl, pH 3.0). Collect fractions for subsequent analysis. The pH of each fraction can be adjusted to neutral by adding 50µL of Neutralization Buffer (1M Tris; pH 9) per 1mL of collected eluate. Pool fractions of interest and exchange into an appropriate storage buffer by desalting or dialysis.

Cells lines

All the cell lines were purchased from ATCC. Mycoplasma analysis was performed before every experiment. Suspension growth: U937 (human histiocytic lymphoma); THP-1 (human acute monocytic leukemia). Culture medium: RPMI-1640 + 10% heat-inactivated FBS + 1% L-glutamine. Culture conditions: 37°C, 5% CO2, humidified atmosphere.

RNASET2 Knockdown in THP-1 Cells

RNASET2 silencing was carried out by means of Nucleofector technology using a vector expressing an shRNA targeting nucleotides 814 to 832 within the RNASET2 mRNA (Genbank accession no. NM_003730.4).
Oligonucleotide sequences for RNAi were generated with the pSicoOligomaker 1.5 software and subsequently aligned to the human genome sequence (UCSC Genome Browser) to test for specificity. Control scrambled sequences were designed having the same length and GC content as the test sequence, but with no significant match to the database. Sense and antisense oligonucleotides representing RNASET2-targeting sequence were annealed and cloned into HpaI/XhoI-digested pSicoR vector (provided by F. Nicassio, Fondazione Istituto FIRC di Oncologia Molecolare, Milan, Italy). The recombinant shRNA-expressing vector was stably transfected into THP-1 cells with the Cell Line Nucleofector Kit V (Amaxa).
The efficiency of RNASET2 knockdown was evaluated by Western blot analysis before every experiment. Cells were maintained under selection throughout all the experiments to ensure the stability of the pool.

Differentiation and polarization protocol of THP-1 cells

For differentiation seed 1.3*10^6 cells in each well (MT6) with RPMI, 10% FBS (decomplemented), 1%Gln, 0.3 µg/mL puromycin, 5 ng/ml PMA. Incubate for 48 h in humidified incubator (37°C, 5% CO2); During the process of differentiation verify the morphology of the cells.
For polarization discard the medium, wash 3 times with PBS and add fresh medium (RPMI + 5 % FBS (decomplemented) + 1 % L- Gln + 0.3 µg/ml puromycin) with the polarizing stimuli:

- M1 : 100 ng/mL LPS + 20 ng/mL INF gamma (2*10^5 IU/mg)
- M2 : 20 ng/mL IL-4 (5*10^6 IU/mg)

Incubate for 24 hours in humidified incubator (37°C, 5% CO2) then proceed with total RNA extraction (Qiagen).

Quantitative real time PCR

Total RNA was extracted was subjected to DNase treatment and was reverse transcribed with random hexamers using the High-capacity cDNA RT kit (Applied Biosystems). Primer sequences were designed with the Primer express program (Applied Biosystems). Real-time RT-PCR was performed on ABI PRISM 7000 with the Power SYBR-green PCR Master Mix (Applied Biosystems), following the manufacturer's instructions. Amplification reactions were performed in triplicate. Following a polymerase activation step at 95°C for 10 minutes, samples were denatured at 95°C for 15'' and annealed/extended at 60°C for 1 minute, for 40 cycles. Fluorescent signals generated during PCR amplification were monitored and analyzed with ABI PRISM 7000 SDS software (Applied Biosystems). The amount of target RNA, normalized to the endogenous reference gene, was calculated by means of log2 of expression level using 35 cycle as LOD.

RESULTS

The experimental results produced during my PhD activities are as follows:

Recombinant human RNASET2 protein purification

Experimental evidence gathered in our group reported that the RNASET2 gene acts as a tumor antagonizing gene in an ovarian cancer model and that this role is not dependent on the catalytic activity of the protein [Acquati, 2005] [Acquati, 2011]. Moreover, our data strongly supported the hypothesis that RNASET2-mediated tumor suppression is carried out in the context of the cancer microenvironment. Indeed, the recruitment and activation of cells belonging to the monocyte-macrophage lineage were shown to be crucial for the observed in vivo oncosuppressive role of RNASET2 [Acquati, 2011] [Acquati, 2013].

In order to further investigate the mechanisms of RNASET2-mediated tumor suppression, the role of this protein in establishing a functional cross-talk between cancer cells and the tumor microenvironment must be thoroughly investigated. To shed light on these issues, the availability of highly pure recombinant RNASET2 protein is an essential requirement.

To this purpose, we already had developed a protocols for expression and purification of recombinant RNASET2 protein in two different heterologous expression systems: the yeast Pichia pastoris and the baculovirus/insect cells system (BEVS) [Campomenosi, 2011]. In both systems, a catalytically competent RNASET2 protein was produced, with comparable levels of expression (about 30 mg of protein/l of conditioned medium). The P. pastoris system proved to be more advantageous, being more cost-effective with respect to BEVS and allowing an easier purification of the protein by affinity chromatography from a protein-free supernatant [Campomenosi, 2011]. However, a full exploitation of this research tool was precluded by several limitations inherent to both systems, such as:

- protein heterogeneity (mostly in the BEVS derived material) due to high molecular weight species (mostly host cell proteins) co-eluting with the RNASET2 molecule;
- a significant loss of the recombinant protein in both flow-through and wash fractions during affinity purification steps;
- the presence of both mildly (38–45 kDa) and highly (50–80 kDa) glycosylated forms of the protein in the eluted fractions (mainly in RNASET2 preparations from P. pastoris);
- the occurrence of endotoxin contamination, which precluded the use of the recombinant protein in functional assays to be carried out with cells from the monocyte/macrophage lineage, which likely represent the most relevant target of the RNASET2 protein in vivo.

To overcome the listed limitations, we decided to focus our efforts on improving the Pichia pastoris system which was much easier to handle in our group in term of available facilities.

The previous system used a strain of Pichia Pastoris (X33) transformed with a plasmid (pPICZ alpha A). The construct code for the human wild type protein RNASET2 tagged with tail of six His (6XHis tag) at the C-terminus (wt_RNASET2-His) and the purification process rely only on an Ion Metal Affinity Chromatography (IMAC) step. The main problems with this system is:

- A significant amount of protein (45%) is lost in the Flow Trough (FT) (tab1).
- The eluate is contaminated with endotoxin.
- The eluate in not homogenous and if it is treated with a polishing step (Size Exclusion Chromatography SEC) in order to remove the higher molecular weight, the recovery of protein drop to 26% of the input (fig 1) (tab1).

Table 1 Comparison of IMAC, SEC, and negative-mode IEX for purification of the RNASET2 proteins from *P. pastoris*

Chromatography	*P. pastoris*			
	wt_RNASET2-His (39 mg/l)[a]			
	Loaded protein (mg)	Eluted protein (mg)	Relative yield (%)	Total yield (%)
IMAC	19.0	10.5[a]	55	55
SEC	10.5	5.0[b]	48	26
IMAC	19.0	10.5[a]	55	55
IEX	10.5	9.9[b]	95	52

a Concentration of the RNASET2 proteins in conditioned media and IMAC eluates was determined by densitometric analysis of the corresponding immunoblots
b Concentration of the RNASET2 proteins from SEC and IEX was determined by spectrophotometry

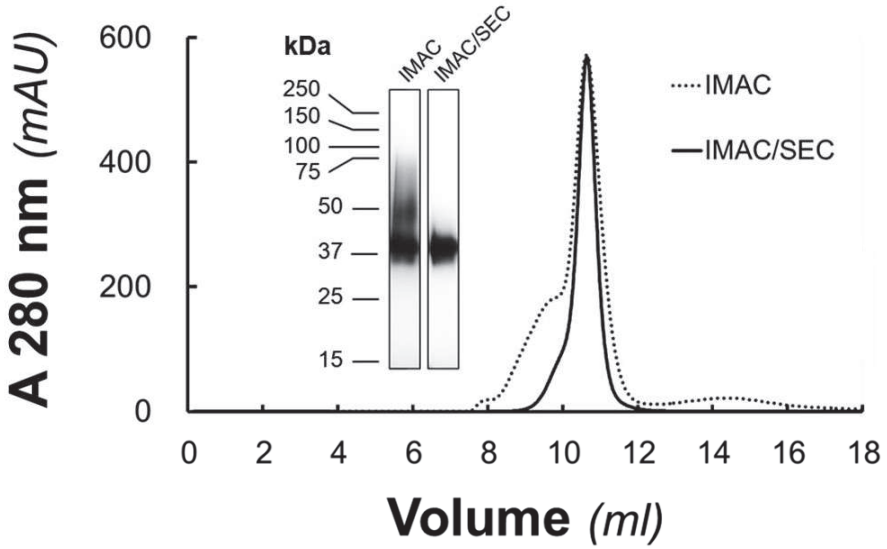

Figure 1. SEC of wt_RNASET2-His from *P. pastoris*. Conditioned media from *P. pastoris* expressing wt_RNASET2-His were passed through Ni-NTA agarose columns manually equilibrated and eluted as described in *Materials and Methods*. Affinity isolated protein from *P. pastoris* was further separated on a Superdex 75 (10 x 300 mm) column using an ÄKTA Purifier FPLC system and chromatograms were recorded as UV absorbance at 280 nm (IMAC, dotted lines). wt_RNASET2-His containing fractions were pooled, concentrated and re-chromatographed on the same SEC column (IMAC/SEC, solid lines). IMAC- and IMAC/SEC- purified protein was run on 10% gels under denaturing and reducing conditions. Representative silver-stained gels are shown (1 mg of total proteins/lane).

Our first attempt to improve the system was try different conditions in the purification protocol. In particular, we performed an IMAC without stringent washing steps (even avoiding more stringent washing steps we didn't manage to achieve a better recovery) follower by a negative Ion Exchange Chromatography (IEX) as a polishing step (fig 2). The IEX was a better solution rather than SEC in term of percentage of recovery (tab1) but still we were not satisfied by the loss in the FT (tab1)

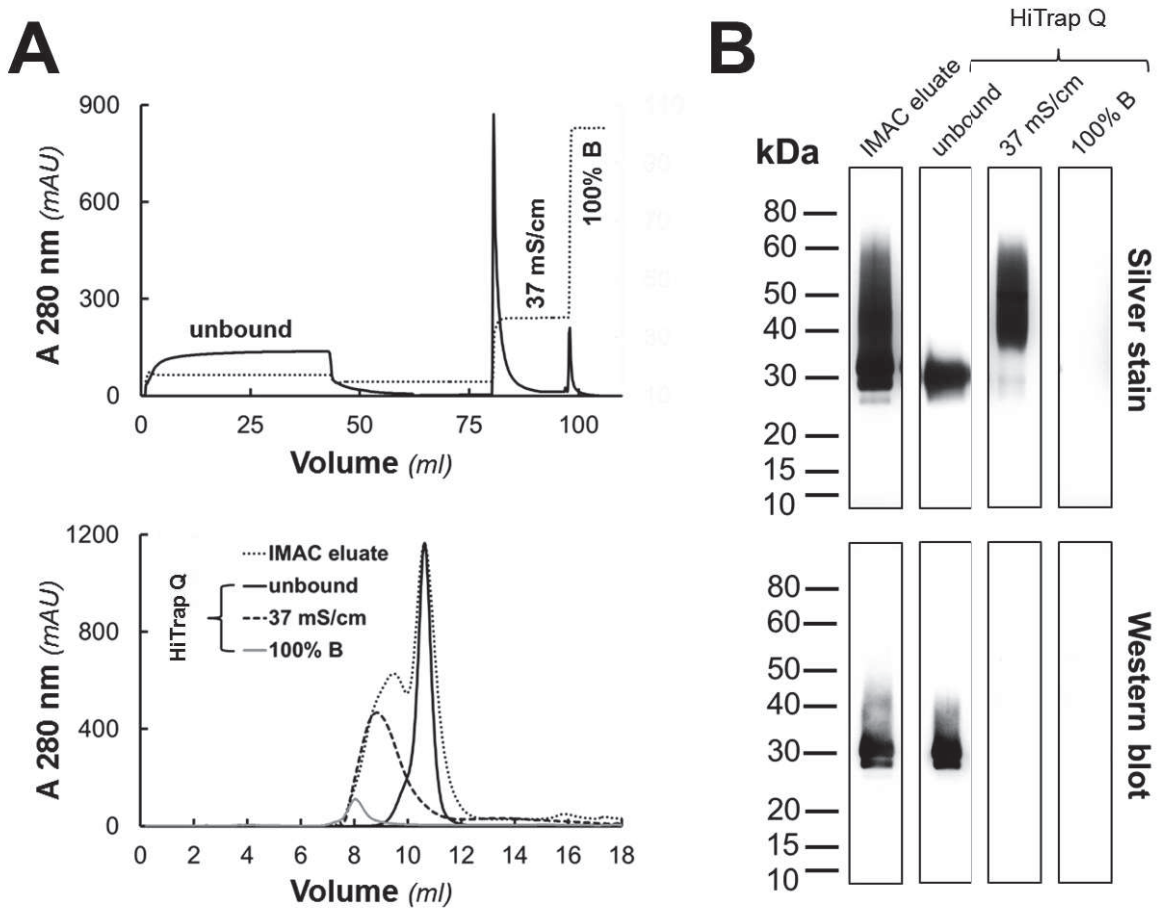

Figure 2. Negative-mode IEX of wt_RNASET2-His from *P. pastoris*. A) wt_RNASET2-His was isolated from *P. pastoris* conditioned medium by HisTrap HP (1 ml) columns and further purified on HiTrap Q XL (1 ml) columns by negative-mode anion exchange chromatography. A representative IEX chromatogram is shown where UV absorbance at 280 nm and mobile phase conductivity are reported as solid and dotted lines, respectively (upper panel). Unfractionated material (IMAC eluate), and HiTrap Q fractions (unbound, 37 mS/cm and 100% B) were analyzed on a Superdex 75 (10 x 300 mm) column. An overlay of the corresponding UV profiles at 280 nm is shown (lower panel). **B**) The same fractions were run on 4-12% gradient gels under denaturing and reducing conditions. Proteins were revealed by either silver staining (upper panel) or western blotting (lower panel), using an anti-His monoclonal antibody (1 mg ad 200 ng of total proteins/lane, respectively).

Considering that most of the protein was lost in the FT and even "playing" with the binding condition didn't help in achieving a better performance, we decided to improve the system by adding another 6XHis tag to the N terminus of the protein (wt 2tag_RNASET2-His) (fig 3).
We decided to keep the X33 as P. pastoris strain as host (X33 was already selected as a good strain for the production of RNASET2; considering the minor modification added by the new tag we decided not to explore the performances of other strains) and to clone the new construct (produced by PCR with ad hoc

primers) in the same pPICZ alpha A vector. After transformation, selection and screening we set up a small batch production and performed a comparative IMAC (fig 3) (for detail on cloning, transformation, selection and screening see Material and Methods). With this new system we managed to achieve a recovery of 95% of the input protein compared to the former 55% using the same IMAC protocol (tab 2).

A

wt_RNASET2-His

DKRLRDNHEWKKLIMVQHWPETVCEKIQNDCRDPPDYWTIHGLWPDKSEGCNRSWPFNLEEIKDLLPEMRAYWPDVIHSFPNRSRFWKHEWEKHGTCAAQVDALNSQKKYFGRSL
ELYRELDLNSVLLKLGIKPSINYYQVADFKDALARVYGVIPKIQCLPPSQDEEVQTIGQIELCLTKQDQQLQNCTEPGEQPSPKQEVWLANGAAESRGLRVCEDGPVFYPPPKKTKHYPYDV
PDYA**HHHHHH**

wt 2tag_RNASET2-His

EF**HHHHHH**DKRLRDNHEWKKLIMVQHWPETVCEKIQNDCRDPPDYWTIHGLWPDKSEGCNRSWPFNLEEIKDLLPEMRAYWPDVIHSFPNRSRFWKHEWEKHGTCAAQVDALNS
QKKYFGRSLELYRELDLNSVLLKLGIKPSINYYQVADFKDALARVYGVIPKIQCLPPSQDEEVQTIGQIELCLTKQDQQLQNCTEPGEQPSPKQEVWLANGAAESRGLRVCEDGPVFYPPPK
KTKHYPYDVPDYA**HHHHHH**

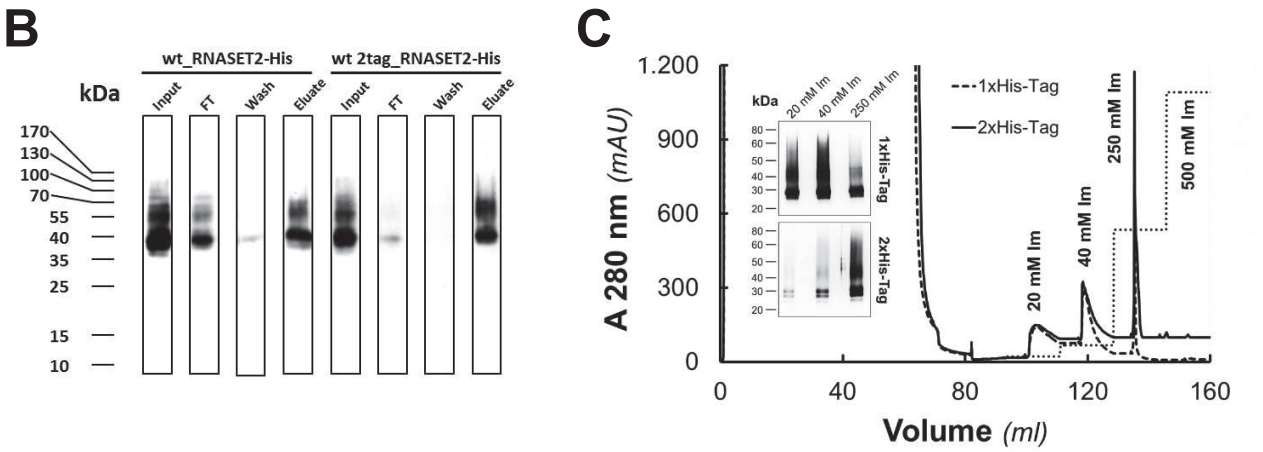

Figure 3. IMAC of wt_RNASET2-His and wt 2tag_RNASET2-His. A) Schematic representation of both single-tagged and double-tagged wild-type RNASET2 protein sequences. In bold the 6xHis tag. CASI site is underlined; CASII site is in red. **B)** WB analysis with polyclonal anti-RNASET2 antibody. Both wt_RNASET2-His and wt 2tag_RNASET2-His were purified from *P. pastoris* conditioned medium, using Ni-NTA agarose beads by gravity-flow. Fractions collected from every step were loaded. The volume of sample loaded was normalized against the final volume of each fraction. **C)** Conditioned media from *P. pastoris* expressing either wt_RNASET2-His or wt 2tag_RNASET2-His were passed through a HisTrap HP (1 ml) column operated with an ÄKTA Purifier FPLC system. Recorded chromatograms are reported as dashed (1xHis-Tag) and solid (2xHis-Tag) lines, respectively. The dotted line indicates concentration of the eluent buffer (%B). Fractions eluted with 20, 40 and 250 mM imidazole were normalized by volume and run on 4-12% gradient gels under denaturing and reducing conditions. Representative silver-stained gels are shown in the inset.

Table 2 Comparison of IMAC purification of wt_RNASET2-His and wt 2tag_RNASET2-His from *P.*

Fraction	Band density (AU)	Loaded volume (µl)	Total volume (µl)	Total density (AU)	Protein amount (µg)	Protein yield (%)
wt_RNASET2-His (11.7 mg/l)[a]						
Input	120,561	2.50	9,000	4.3E+08	584	100
FT	38,937	2.50	9,000	1.4E+08	189	32
Wash	3,005	0.56	2,000	1.1E+07	15	2
Eluate	66,073	0.22	800	2.4E+08	320	55
wt_2tag_RNASET2-His (9.9 mg/l)[a]						
Input	80,616	2.50	9,000	2.9E+08	495	100
FT	3,277	2.50	9,000	1.2E+07	20	4
Wash	0	0.56	2,000	0.0E+00	0	0
Eluate	79,209	0.22	800	2.9E+08	486	98

a Conditioned media (50 ml) were concentrated to a final volume of 9 ml (~5.6 fold) prior to IMAC. The values here reported refer to protein concentration in the non-concentrated media, as determined by densitometric analysis.

The new developed system provides a significant increase in term of performance. Moreover, by placing the chromatography system under sterile condition, sanitizing all the lines and working with LPS tested buffers (or buffers cut with 10 kDa filters) throughout all the steps we managed to drop the LPS contamination of the purified protein to 0.003 EU/100 ug RNASET2 (0.3 pg LPS/ 100 ug RNASET2).
Considering the use of metal chelating resins during the purification steps, we decided to test the end-product protein preparation for contamination of Ni, Cd and Zn by Atomic Adsorption Spectroscopy (AAS). For all the metals the concentration was below the limit of detection of the instrument.
The low endotoxin content and absence of contamination by metals are important features, especially considering the plan of studying the role of RNASET2 in macrophages polarization.

Finally, the proper folding of the new recombinant human RNASET2 produced (wt 2tag_RNASET2-His) was checked by means of a zymogram (exploiting the ribonuclease activity of RNASET2) (fig 4). A catalytically inactive form of the protein (already developed in our laboratory) was used as negative control (H65/118F_RNASET2-His).

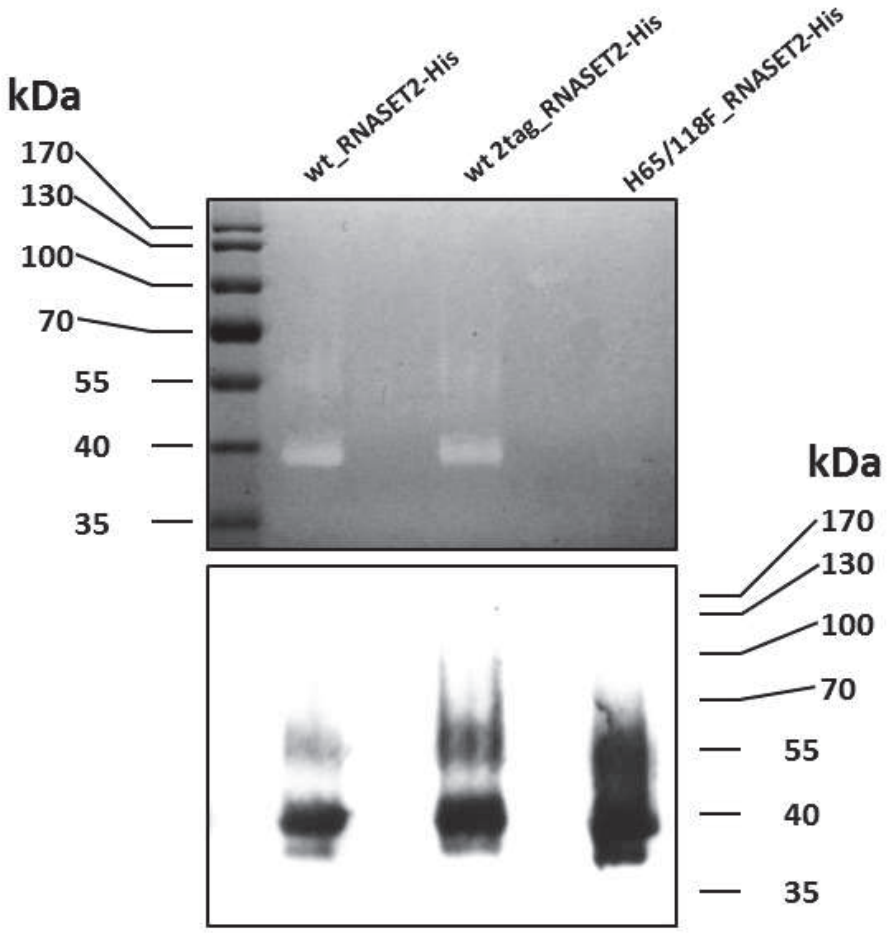

Figure 4. Zymographic analysis of the catalytic activity of wt 2tag_RNASET2-His. Upper panel: zymography was performed using total RNA from Torula yeast as substrate. 600 ng of recombinant protein/lane were loaded. The activity of both wt 2tag_RNASET2-His protein was compared to that of the single-tagged wt RNASET2 protein (wt_RNASET2-His). The catalytically-inactive mutant was loaded as negative control (H65/118F_RNASET2-His). **Lower panel**: the identity of the bands which showed ribonucleolytic activity was confirmed by immunodetection with polyclonal anti-RNASET2 antibody.

Analysis of the evolutionary conserved relationship between RNASET2 and immune cells

T2 RNases represent one of the most widespread class of RNases, being found in viruses, bacteria, protozoans, plants and metazoans [Luhtala, 2010]. This feature, coupled to their rather unspecific substrate preference (they usually cleave RNAs at all four bases), suggest the occurrence of one or more ancient, evolutionarily relevant roles for T2 RNases.

As already mentioned, several studies have reported the widespread tumor suppressive role for several members of the T2 RNase protein family and the recruitment of immune cells seems to be the one of the

main causes of this suppression [Smirnoff, 2006; Schwartz, 2007; Acquati, 2011, 2013] nevertheless, we don't understand yet the mechanism behind this effect.
In order to improve our knowledge of these functional features of T2 RNases and at the same time to evaluate their evolutionary conservation, we tested the role of human recombinant RNASET2 in the activation and recruitment of immune cells using as experimental model the Hirudo Verbana, a medicinal leech species closely related to Hirudo medicinalis.
Hirudo is a consolidated experimental animal model for several reasons:

- It represents a suitable tool for experimental manipulation, being cost-effective, easy to handle and devoid of significant ethical considerations in relation to its use and regulatory restrictions.
- The main immune response processes in leeches have been shown to be strikingly similar to those reported in vertebrates, since they involve similar cellular mechanisms and a common equipment of key molecules playing pivotal roles for regulating hematopoietic cells activation and differentiation.
- Any response evoked in leeches by a wide range of different stimuli is activated within a short period of time (6–24 h) and is clearly and easily detectable due to the small size and anatomical features of this experimental model [de Eguileor, 1999, 2003, 2004; Grimaldi, 2004, 2006; Tettamanti, 2004; Girardello, 2015a, b; Schorn, 2015b].
- The use of the biopolymer Matrigel (MG), once soaked with the molecule subject of the study, allows to investigate several key aspects of the immune response in leeches, making it possible to isolate and further characterize specific cell type [Grimaldi, 2008, 2009, 2011; Girardello, 2015a].

In order to evaluate the putative role of RNASET2 in the regulation of innate immune response in Hirudo, in particular in the activation and migration of macrophages, we first assessed the effects of recombinant human RNASET2 (rRNASET2) injection in the leech body wall. To this aim, morphological and immunohistochemical analyses were carried out on leech tissue sections from uninjured, PBS-injected, rRNASET2- injected (with or without preincubation of the recombinant protein with an anti-RNASET2 antibody) and LPS-injected animals. The same analyses were also carried out on rRNASET2- soaked, polymerized matrigel pellets explanted from the leech body wall after implantation for 1 week.

The body wall of unlesioned (fig 5 a) or PBS-injected (fig 5 b) leeches showed a typical cutaneous muscle sac, formed by epithelium and muscle fibers arranged in groups and surrounded by a loose connective tissue. In the body wall of these control animals, a few non-muscle cells were immersed in the connective tissue surrounding the muscles. By contrast, at 24 h (fig 5 c) and 1 week (fig 5 d, e) following rRNASET2 injection, a large number of infiltrating cells was clearly detected underneath the epithelium and in the connective tissue surrounding the muscle fibers. A marked reorganization of the muscle layers in rRNASET2-treated animals was also evident at the injection site, since the distance between single muscle fields appeared to be greatly increased, due to the infiltration of several cells interposed between them. This cell infiltration process was closely associated with a massive reorganization of the connective tissue and the appearance of new blood vessels in the space between the muscle fields (fig 5 c–e). By contrast, in uninjured (fig 5 a) and PBS injected control leeches (fig 5 b) or in leeches injected with rRNASET2 previously pre-incubated with the antiRNASET2 antibody (fig 5 f–h), muscle fields were in close reciprocal contact and both the infiltration of cells and the appearance of vessels between the groups of muscle fibers or underneath the epithelium were negligible (fig 5 f–h).

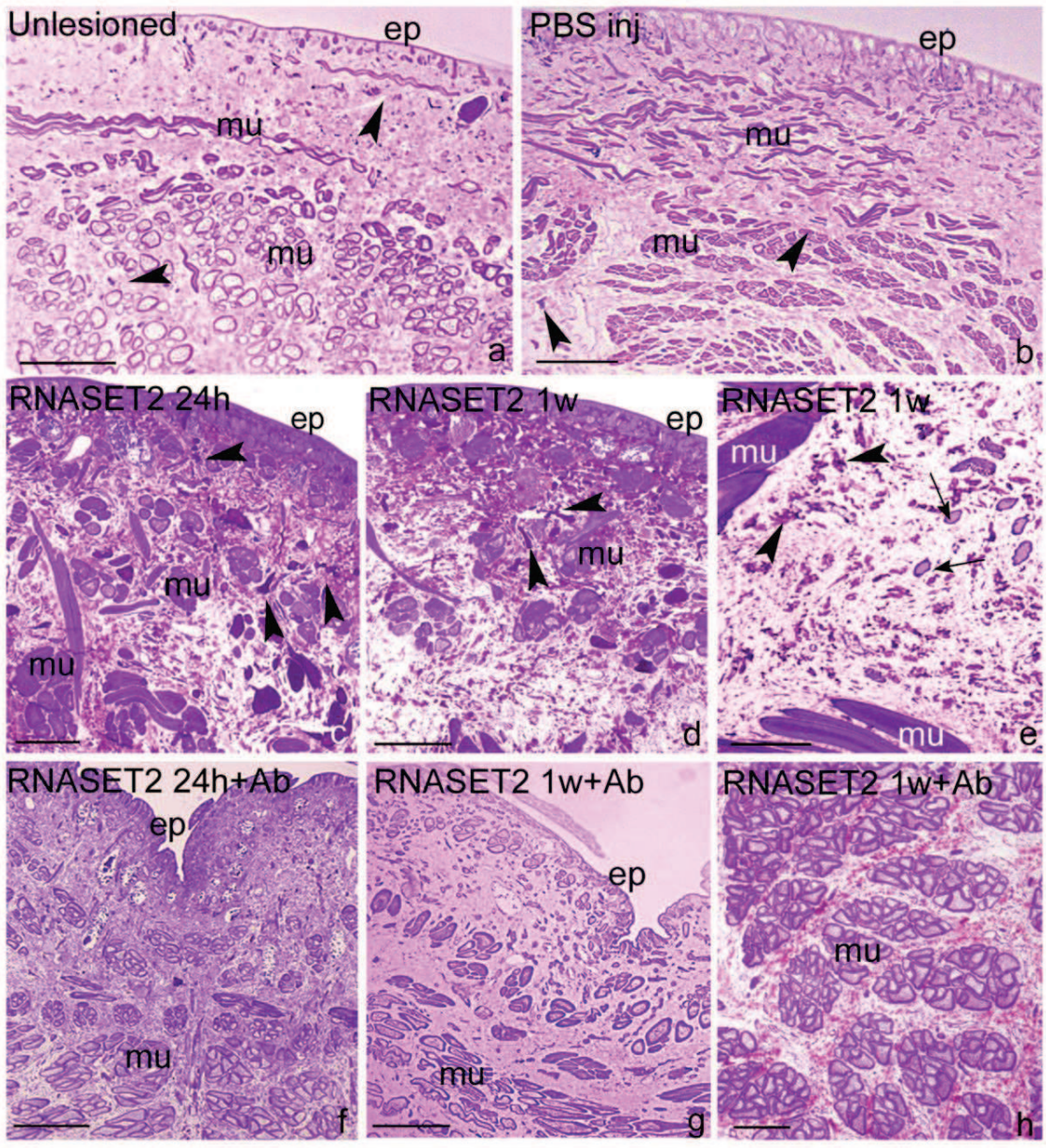

Figure 5. Light microscope morphological analysis of leech body wall sections. In unlesioned (a) and PBS-injected (b) animals, a few cells (arrowheads) among muscle fibers are visible; 24 h (24h, c) and 1 week (1w d, e) following rRNASET2 injection, numerous migrating cells (arrowheads) and neovessels (arrows) are visible. Injection of rRNASET2 pre-incubated with the neutralizing anti-RNASET2 antibody (Ab) significantly reduces both cell migration and neo vessel formation (f–h). mu muscles; ep epithelium. Bars 100 µm.

Ultrastructural TEM analysis of unlesioned (fig 6 a) or PBS-injected (fig 6 b) leeches confirmed that muscle fibers forming the muscular fields were very close to each other and the extracellular matrix surrounding them was scant and devoid of cells. By contrast, 24 h (fig 6 c, d) and 1 week (fig 6 e, f) following rRNASET2 injection, clearly recognizable neovessels were observed underneath the epithelium, with the vessels lumen containing circulating cells. The observed angiogenic process displayed the typical features of an inflammatory response-derived process [Grimaldi, 2006], with circulating cells extravasating and migrating into the nearby connective tissue and thereby differentiating into mature leukocytes, likely involved in the leech innate immune response. Indeed, a high prevalence of cells displaying the typical appearance of macrophages was detected in the extracellular matrix underlying the epithelium (fig 6 c) and surrounding the muscle fibers of rRNASET2-treated animals (fig 6 d, e). These cells were clearly distinguishable by an elongated shape, an irregular membrane (likely involved in the formation of pseudopodia, a typical feature of cells involved in active migration) (fig 6 e) and a cytoplasm with a large nucleus and a few electron-dense granules (fig 6 d). Besides the infiltration of immunocompetent cells, rRNASET2-treated leeches were also characterized by a massive fibroplasia across the entire body wall.
As in vertebrates, leech fibroblasts are responsible for the synthesis and remodeling of the extracellular matrix [Tettamanti, 2005]. These cells were easily recognizable by TEM analysis in rRNASET2-injected animals due to their tapered shape and the presence of several lipid droplets in their cytoplasm. Moreover, the fibroblasts' cell membrane was characterized by the presence of laminar projections, known to be involved in the formation of a cellular microenvironment that promotes fibrillogenesis (fig 6 f). As already observed by optical microscope analysis, the number of vessels and immunocompetent cells underneath the epithelium and between the groups of muscle fibers was very scant in animals injected with rRNASET2 that was pre-incubated with anti-rRNASET2 neutralizing antibody, (fig 6 g, h), suggesting that the observed tissue morphological changes represent a specific effect of rRNASET2 treatment.

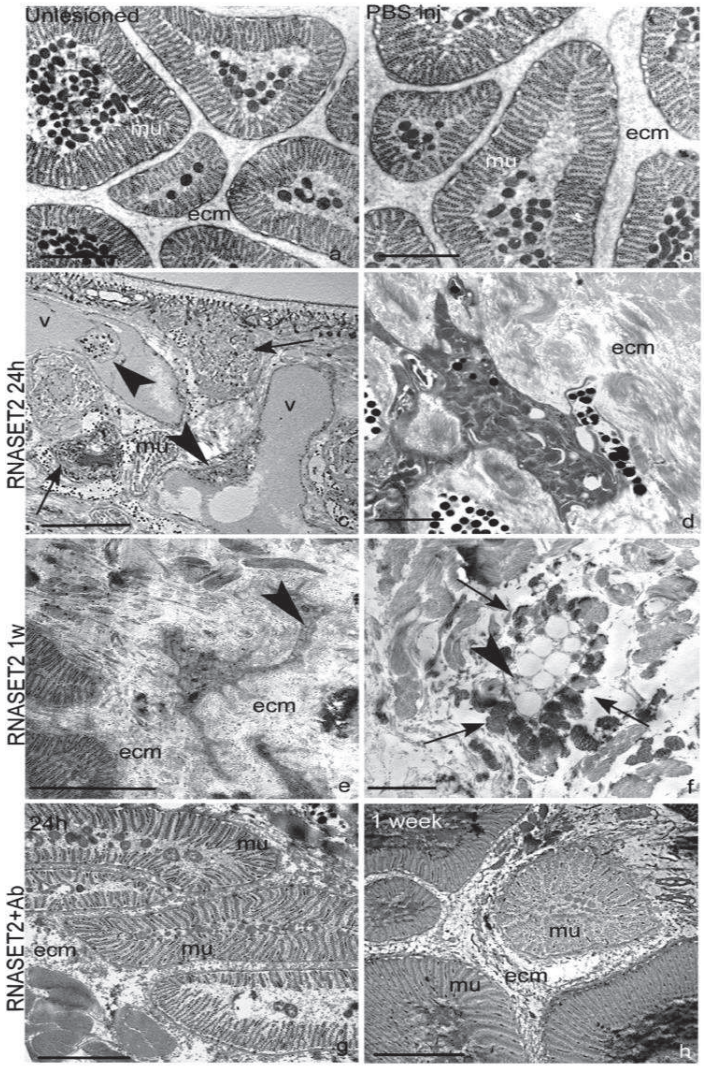

Figure 6. Ultrastructural analysis at TEM of leech body wall. details of a group of muscle fibers (mu) in unlesioned (a) and PBS-injected (b) leeches. Muscle fibers (mu) are close to each other and surrounded by scant extracellular matrix (ecm) devoid of cells. After 24 h from rRNASET2 injection (c, d), macrophages (arrows) and vessels (v) containing circulating cells (arrowheads) are visible underneath the epithelium. After 1 week from rRNASET2 injection, migrating macrophages (arrowhead in e) and fibroblasts (arrowhead in f) in active fibrillogenesis (arrows) are observable (e–f). The number of vessels and macrophages is highly reduced in rRNASET2 preincubated with anti-rRNASET2 Ab injected leeches (g, h). Bars (a–c, e, g, h) 5 µm, (d, f) 2 µm.

In order to better define the cell types recruited in leech tissues following rRNASET2 injection and thus confirm the occurrence of a RNASET2-driven inflammatory response, immunofluorescence (IF)

experiments were performed on tissue cryosections from unlesioned, PBS-injected and rRNASET2- injected animals. Recombinant RNASET2-treated sections were investigated at both 24 h and 1 week, with and without neutralizing anti-RNASET2 antibody pretreatment (figs 7 a– p; 8 a–d).
Immunohistochemical assays were carried out with an anti-HmAIF-1 antibody, a known marker for leech macrophages [Drago, 2014; Schorn, 2015a, b]
By these assays, HmAIF-1 turned out to be constitutively expressed at a low level in the body wall of uninjured animals. The protein was mainly detected in a few cells located in the connective tissue underlying the epithelium and surrounding the muscle fibers fields (fig 7 a, b). The same expression pattern was observed in the samples analyzed 24 h (fig 7 e, f) after PBS injection, suggesting that the mechanical stress induced by injection of a saline solution did not affect significantly the expression of HmAIF-1 in the leech body wall.
By contrast, a highly increased number of HmAIF-1+ migrating cells were clearly recognizable 24 h (fig 7 i, j) and 1 week (fig 8 a) after rRNASET2 injection. These cells were mainly located under the epithelium and among muscle fibers. Strikingly, 24 h (fig 7 m, n) and 1 week (fig 8 c) from injection with rRNASET2 pre-incubated with the neutralizing anti-RNASET2 antibody, the number of migrating HmAIF-1+ cells was significantly reduced. No signal was detected in the negative control experiments in which the primary antibodies were omitted (fig 7 d, h, l, p).
Taken together, these data are indicative of a strong recruitment of cells belonging to the macrophage lineage at the rRNASET2 injection sites.
Because no previous report of endogenous T2 ribonucleases in leeches are available, we decided to perform an IF with the antihuman RNASET2 antibody, over the same sections investigated for HmAIF-1.
Interestingly, we observed a positive signal that seems to follow the same pattern of HmAIF-1, being constitutively expressed at low level in the untreated and PBS injected samples (fig 7 a, c, e, f) and overexpressed after rRNASET2 injection (fig 7 k, fig 8 b) but not if pre-incubated with the neutralizing anti-RNASET2 antibody (fig 7 o; fig 8 d).
This result suggest that the antihuman RNASET2 antibody might be able to detect a putative T2 ribonuclease in leeches and this protein seems to follow the HmAIF-1 pattern of expression.

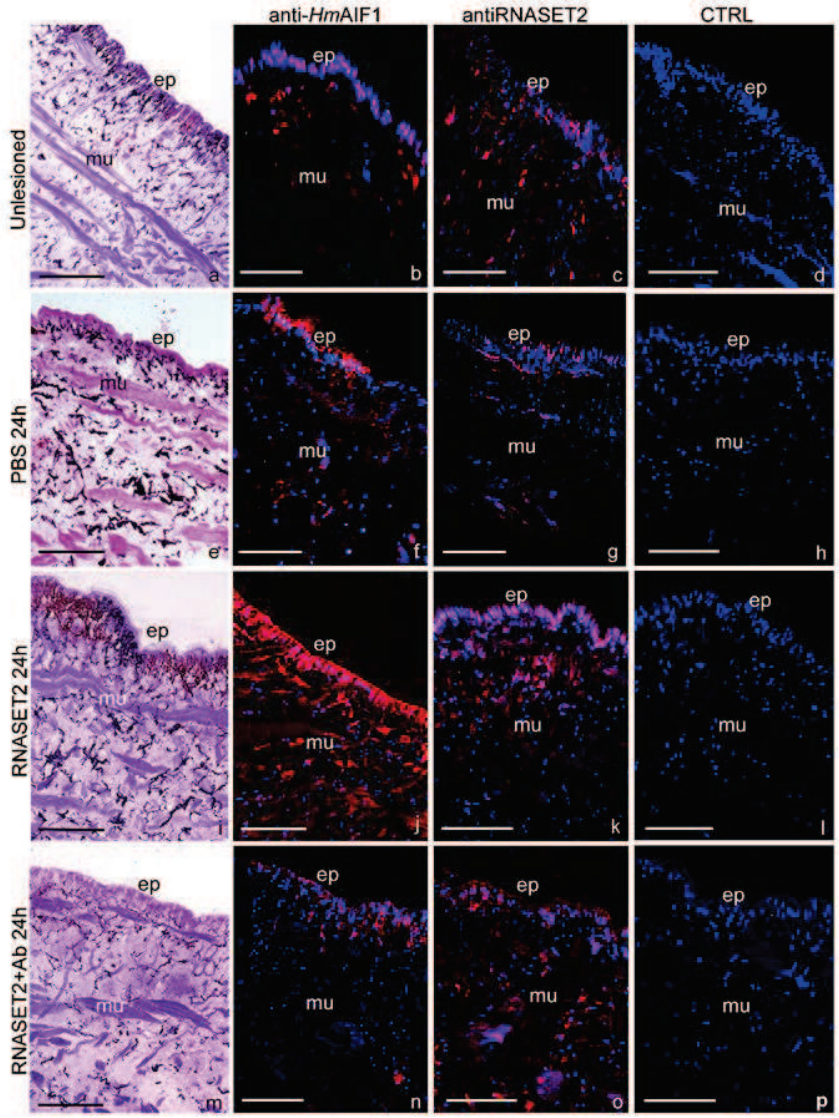

Figure 7. Immunofluorescence analysis of cryosections from medicinal leech body wall. unlesioned (a–c), PBS-injected (e–g), rRNASET2-injected (i–k) and neutralizing antibody preincubated rRNASET2-injected animals (m–o). The anti-HmAIF-1 and anti-RNASET2 antibodies stain in red a few cells among muscle fibers (mu) and underneath the epithelium (ep) in unlesioned, PBS-injected and antiRNASET2-neutralized, rRNASET2 injected leeches, whereas several migrating immune-responsive cells located under the epithelium (ep) and among muscles (mu) are detected 24 h following RNASET2 injection. No signal is detected in negative control experiments in which the primary antibodies were omitted (d, h, l, p). Cell nuclei stained blue by treatment with DAPI. Bars 100 µm

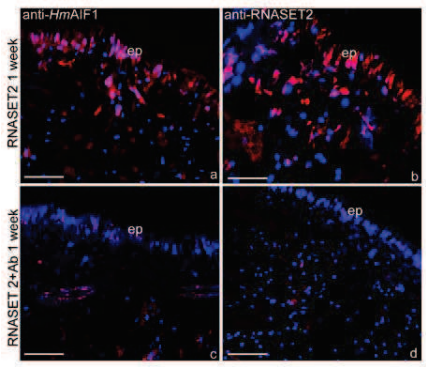

Figure 8. Ultrastructural analysis at TEM of leech body wall. injected with rRNASET2 (a, b) or rRNASET2 pre-incubated with the neutralizing anti-RNASET2 antibody (c, d). One week following injection of RNASET2 alone, several HmAIF-1+ and anti RNASET2+ cells (in red) are mainly located underneath the epithelium (ep). Cell nuclei are stained in blue with DAPI. Bars 50 µm.

To further confirm the ability of rRNASET2 to induce macrophages migration in vivo, recombinant RNASET2 protein was added to MG biopolymer held at a liquid state and the mixture was subsequently inoculated in leeches; the polymer once injected become a sponge that release rRNASET2 and capture recruited cells. This approach provides a better understanding of the effect of rRNASET2 by reducing the complexity of the sample under study (a slice of MG instead of a slice of leech) still maintaining the the salient characteristics of an *in vivo* system.
In order to characterize the cell types infiltrating the polymerized biopolymer, MG solid pellets formed following inoculation were explanted after 1 week and processed for standard histological and immunofluorescence analyses using anti-CD68, anti-HmAIF-1 (both specific for leech macrophages) [Schorn, 2015a, b] and anti-RNASET2 antibodies (fig 9 a–o). In keeping with our previous results, MG samples containing rRNASET2 protein appeared massively infiltrated by elongated and irregularly-shaped cells characterized by numerous cytoplasmic expansions (fig 9 g). These cells were HmAIF-1+ (fig 9 h), CD68+(fig 9 j) and RNASET2+(fig 9 k). A much lower number of infiltrating cells was observed in control MG specimens lacking rRNASET2 (fig 9 a, b), or added with PBS (fig 9 d, e) or rRNASET2 pre-incubated with anti-RNASET2 antibody (fig 9 m, n). No signal was detected in negative control experiments in which the primary antibodies were omitted (fig 9 c, f, i, l, o).

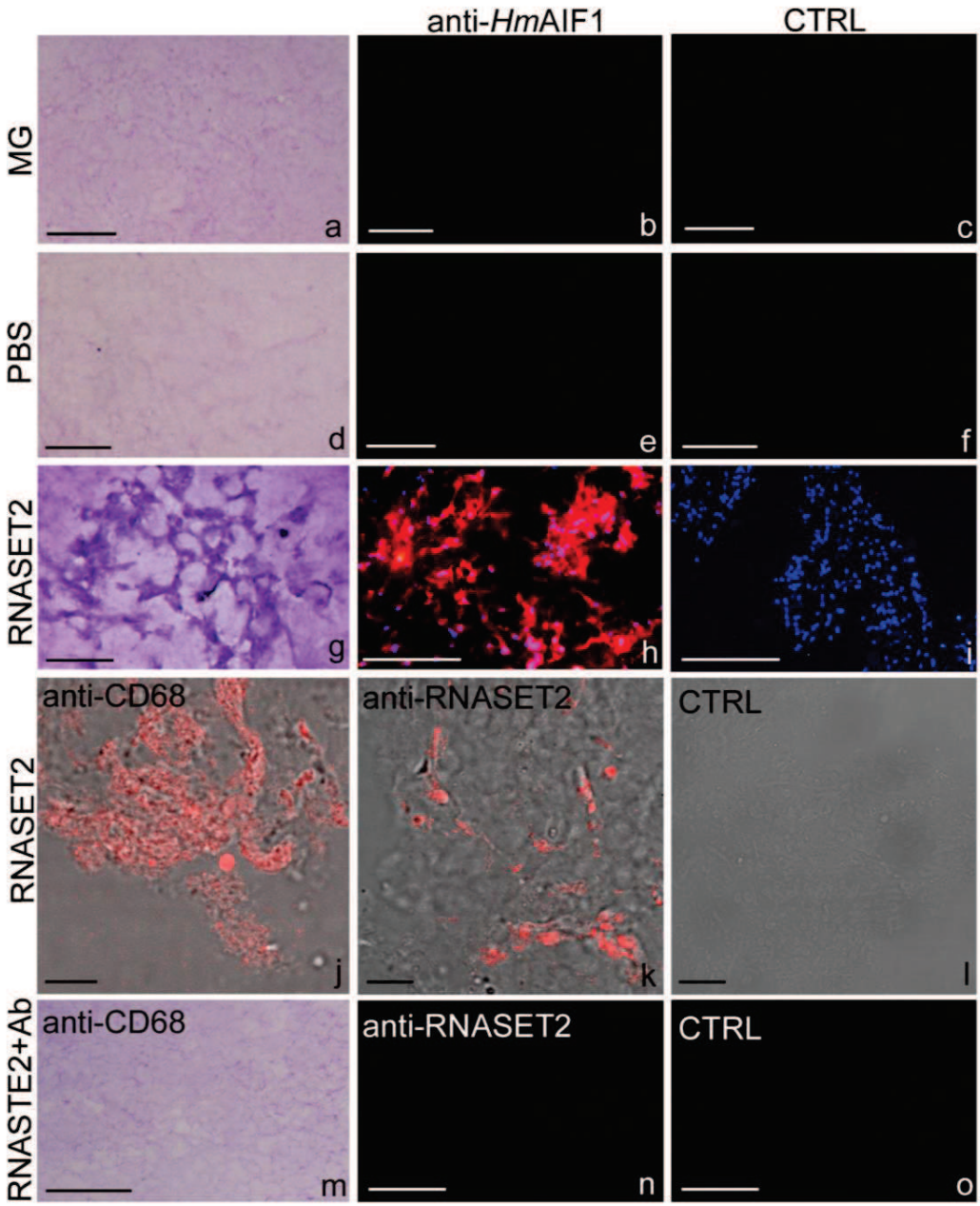

Figure 9. Morphological and immunohistochemical analyses of MG sponges. untreated control MG sponges (a–c) and MG sponges treated with PBS (d–f), rRNASET2 (g–l) and neutralizing antibody-pretreated rRNASET2 (m–o). After 1 week, only MG plugs supplemented with rRNASET2 are highly infiltrated by elongated and irregularly shaped characterized cells and by numerous cytoplasmic expansions (g). These cells are HmAIF- 1+ (h), CD68+ (j) and RNASET2+ (k). Cell nuclei are stained in blue with DAPI (h, i). No signal is detected in negative control experiments in which the primary antibodies are omitted (c, f, i, l, o). Bars (a–i, m–o) 100 µm, (j–l) 10 µm.

We next addressed the putative involvement of rRNASET2 in regulating the inflammatory response following injection with LPS, a well-known strong stimulator of innate immune response in almost all eukaryotic species, ranging from insects to humans. It was already reported that LPS injection promotes a massive migration of macrophages in the body wall of Hirudo [de Eguileor, 1999; Schorn, 2015a]. The immunophenotype of cells involved in LPS-mediated inflammatory response was evaluated by double-labeling with an anti-RNASET2 antibody and anti-HmAIF-1 or anti-CD68 antibodies.

As expected, the assays showed that, unlike unlesioned animals (fig 10 a, b), LPS-injected animals (fig 10 c, d) displayed a marked migration of macrophages that were mainly localized underneath the epithelium and in the connective tissue surrounding the muscle fibers. Strikingly, these infiltrating macrophages were expressing both RNASET2 and CD68. Thus, the massive recruitment of macrophages coupled to upregulation of endogenous RNASET2 that we previously observed following rRNASET2 treatment was recapitulated when leeches were challenged with a strong inflammatory stimulus. Moreover, the cellular source of leech endogenous RNASET2 turned out to be the macrophage cell itself.

To confirm the result observed by IF, the RNASET2 and HmAIF-1 expression pattern of uninjured, PBS-treated, rRNASET2-treated (with and without pre-incubation with the neutralizing antiRNASET2 antibody) and LPS-challenged animals was also evaluated by means of western blot analysis (fig 10 e, f). The injection of the anti-RNASET2 antibody alone was also performed as a further control. The analysis was carried out on protein extracts taken from the leech body wall at the site of injection.

Two main RNASET2-immunoreactive bands of approximately 34 and 29 kDa (the latter being visible only in a subset of the tested samples) were detected in leech tissues (fig 10 e). Of note, a control sample from the human OVCAR3 ovarian cancer cell line (known to express high endogenous RNASET2 levels) also showed two main antiRNASET2-reactive bands, although their molecular masses were slightly different from those observed in leech tissues (we do not have any information on the endogenous leech protein hence the difference in term of migration might be due to differences in term of sequence or post-translational modifications).

By using an anti-AIF-1 antibody, a single band of 18 kDa corresponding to the expected molecular weight for HmAIF-1 [Schorn, 2015a] was detected (fig 10 f). Strikingly, the expression pattern of RNASET2 and AIF-1 turned out to be remarkably similar in most if not all the samples tested and was in keeping with the pattern previously reported by immunofluorescence assays. Indeed, both RNASET2 and HmAIF-1 turned out to be constitutively expressed at a low baseline level in unlesioned, PBS and rRNASET2 plus neutralizing anti-RNASET2 antibody injected animals (fig 10 e, f). In contrast, expression of both RNASET2 and HmAIF-1 was significantly increased in the samples from LPS and RNASET2-injected animals. Moreover, a very weak or undetectable signal was observed in the proteins extract of leech injected with the antiRNASET2 antibody alone (fig 10 e, f), again suggesting the occurrence of a RNASET2-specific effect. Thus, rRNASET2 injection was shown to induce a change in the expression pattern of both proteins that is very similar to that induced by injection with a highly pro-inflammatory agent such as LPS.

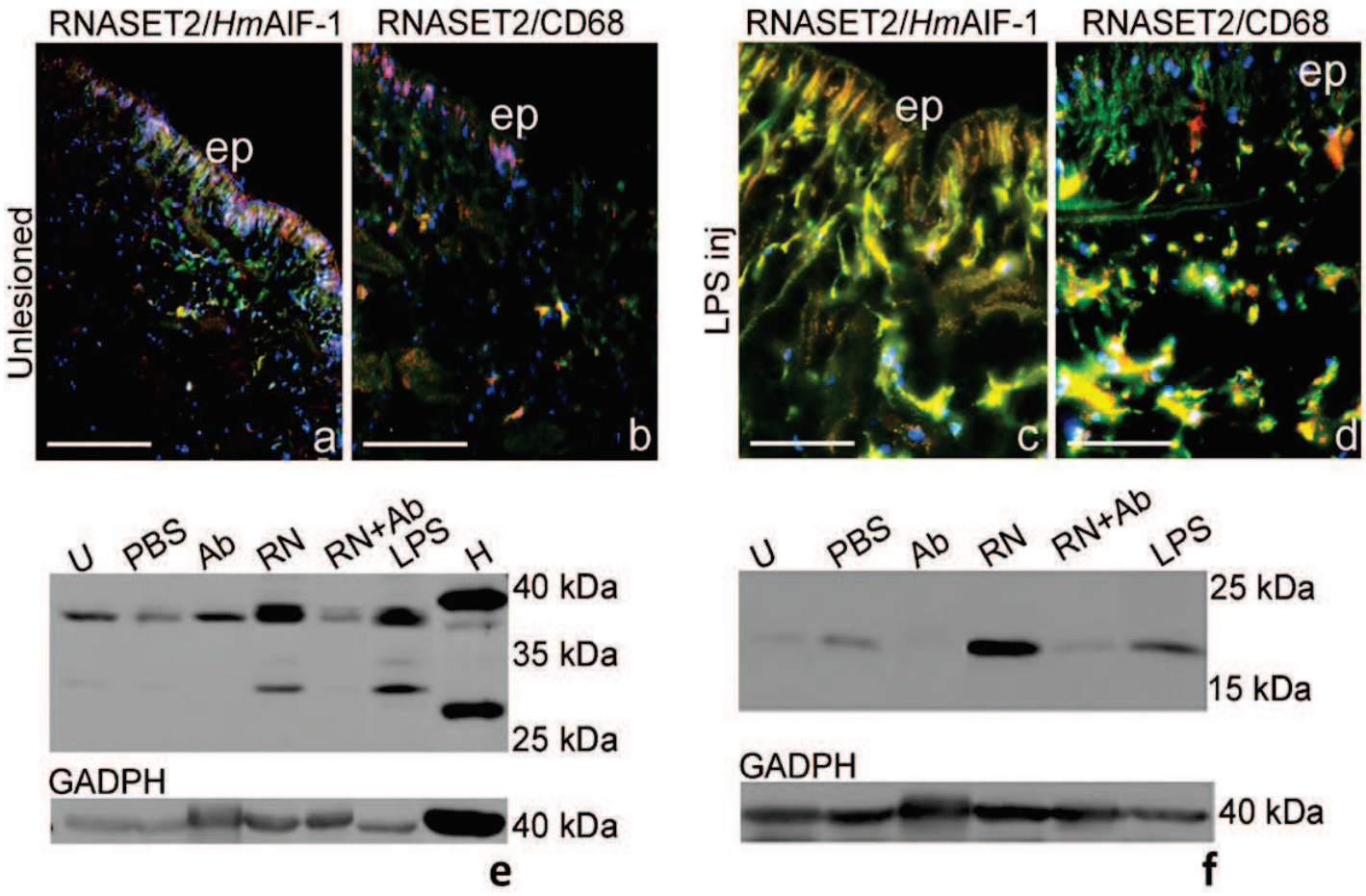

Figure 10. Co-immunolocalization and WB analysis. Double immunolocalization of RNASET2 and HmAIF-1 or RNASET2 and CD68 of unlesioned (a, b), LPS-injected (c, d) leech body wall and western blot analysis (e, f). At 24 h following LPS injection, numerous RNASET2+/HmAIF-1+ and RNASET2+/CD68+ macrophages (yellow) migrating towards the injected area are visible under the epithelium (ep) and among the muscle fibers (mu). Double immunostaining is performed with anti-RNASET2 (red) and anti HmAIF-1 or anti-CD68 (green). No signal is detected in negative control experiments in which primary antibodies are omitted. Nuclei are stained in blue with DAPI. Bars (a–d) 50 µm. e, f Western blot analysis. A protein extract of human OVCAR3 ovarian cancer cell line (H), used as positive control and of body wall biopsies at the injection sites from unlesioned (U), PBS-treated, anti-RNASET2 alone-treated (Ab), rRNASET2-treated (RN), rRNASET2 plus neutralizing anti-RNASET2 antibody (RN+Ab) or LPS-treated leeches were probed with the antiRNASET2 (e) or anti-HmAIF-1 (f) antibodies. The antibody antiRNASET2 recognizes two RNASET2-immunoreactive bands of approximately 34 and 29 kDa in leech tissues and of 36 and 27 kDa in OVCAR3 cell line exctract, while the anti-HmAIF-1 detects in leech tissues a specific immunoreactive band of about 18 kDa, according to the molecular weight ladder (kDa). The housekeeping protein Dglyceraldehyde-3-phosphate dehydrogenase (GAPDH) is used as a loading control. No signal was observed in the proteins extract of leech injected with the Ab alone.

Attempts to identify a putative receptor for RNASET2

Recent experiments carried out in our group demonstrated that RNASET2 is actively internalized by a human cancer cell line [Lualdi, 2015], this finding coupled with the evidence gathered from chemotaxis experiments [Acquati, 2013], allowed us to hypothesized that there could be a membrane-bound interactor for this protein. Therefore, in order to get a better insight of this molecular mechanism we tried several strategies to identify a putative receptor for RNASET2.
The basic idea behind all of our approaches was to try to covalently link RNASET2 (either the endogenous protein or the human recombinant protein) to any interactor and, after purification of the complex, perform a MS analysis to characterize the interactants.
It is important to specify that before proceeding to the purification step we needed to set up an experimental system (composed of a cell line and an assay) which is able to produce a detectable complex. In this sense, the crosslinking should change the apparent molecular weight of the linked interactor, therefore we planned to identify the formation of a complex by monitoring the shift in molecular weight of RNASET2 positive signals by WB.

As the first approach we performed a chemical modification of the purified protein. The modification was made with different NHS-ester diazirines (SDA, LC-SDA, Sulfo-SDA and Sulfo-LC-SDA). These compound are heterobifunctional crosslinkers that contain an amine-reactive N-hydroxysuccinimide (NHS) ester and a photoactivatable diazirine ring. NHS esters react efficiently with primary amino groups in pH 7-9 buffers to form stable amide bonds; the product is a photoactivable protein probe. Exposure of diazirines to long-wave UV light creates reactive carbene intermediates that can form covalent bonds through addition reactions with any amino acid side chain or peptide backbone within the spacer arm distance (1.25 nm for LC-compound and 0.39 nm for non LC-compound).
The modified protein was added to OVCAR3 silenced cells (among a panel of cell lines the latter resulted to be the strongest binder for RNASET2 [unpublished data]; the silenced model ensures that the putative receptor, if present, is not already bound to the endogenous protein) and irradiated with UV light. The protein extract was analyzed by WB but despite several attempt, we could not observe any shift in the molecular weight of RNASET2.

As the second approach we decided to perform metabolic labeling of OVCAR3 cells using two chemical L-Photo-Leucine (Photo-L) and L-Photo-Methionine (Photo-M).
Photo-L and Photo-M are amino acid derivatives that contain diazirine rings for UV photocrosslinking of proteins. These photo-active amino acids substitute for their respective natural amino acids and are incorporated directly into proteins using the endogenous mammalian translation machinery. The overall incorporation rate depends on amino acid frequency, sequence length, protein abundance and protein turnover. Photoactivation of the diazirine rings creates reactive carbene intermediates that irreversibly crosslink proteins generally within protein-protein interaction domains.
In this case we exploited the high RNASET2 endogenous expression of OVCAR3 cell line grown with Photo-L and Photo-M before irradiation and analysis of the protein extract. After several attempt, even exploring different conditions, we didn't manage to observe any shift in the molecular weight of RNASET2, meaning we were not able to produce any detectable complex.

Considering that most of the result obtained show evidence of an interaction between RNASET2 and cells belonging to the monocyte/macrophage lineage, we decided to test the system with a promyelocytic cell line.

In our last attempt we incubated the recombinant human RNASET2 with U937 cell line (a promyelocytic cell line which do not show any detectable expression of endogenous RNASET2) and in order to stabilize the putative complex we used a non UV activable crosslinker (BS3).
BS3 ((bis[sulfosuccinimidyl] suberate) is a water soluble homobifunctional N-hydroxysuccinimide ester (NHS ester), it reacts efficiently with primary amino groups in pH 7 to 9 buffers to form stable amide bonds. The reaction generally involves the side chain of lysine residues and the N-terminus of each polypeptide. As the chemical crosslinkers presented before, BS3 is able to covalently link two or more proteins in close proximity, but in this case there is no need to activate the reaction with UV irradiation.
With this experimental setup we finally managed to see a shift in the molecular weight of RNASET2 by WB (fig 11 a), but unfortunately, despite several attempts, once we moved to the purification step we didn't manage to elute any complex (Fig 11 b).

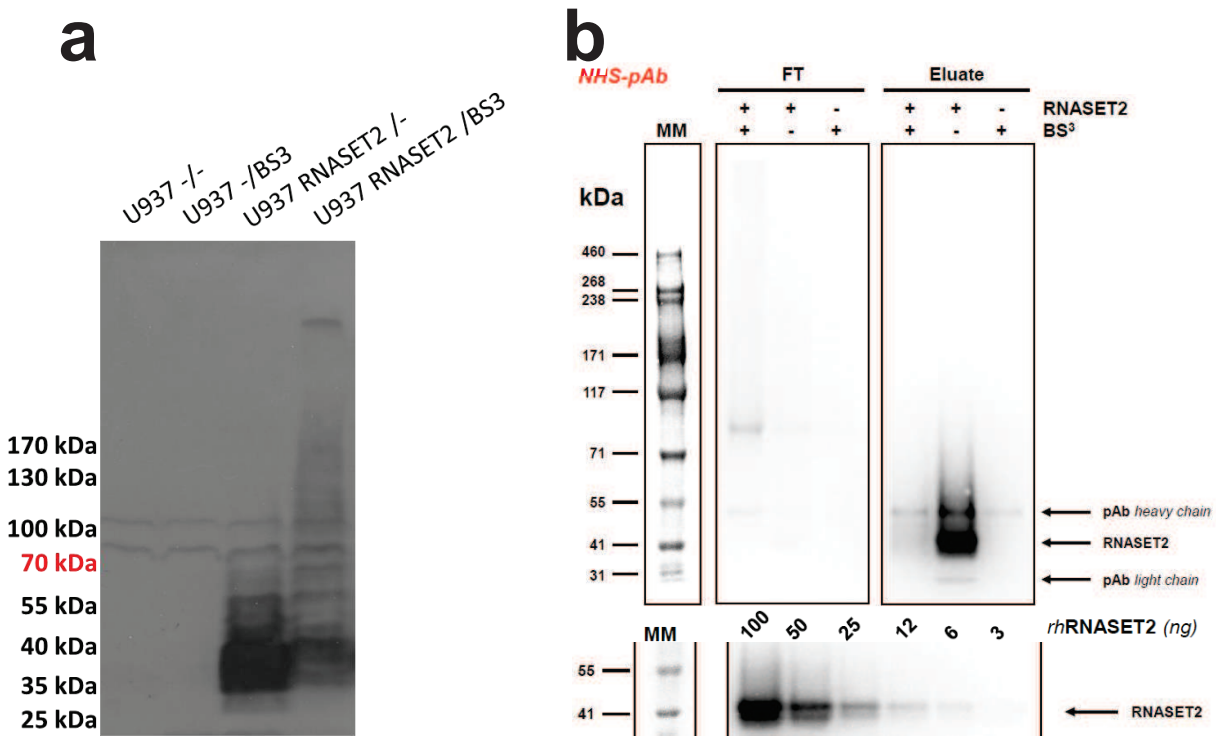

Figure 11. WB analysis for the identification of the putative RNASET2 receptor (anti-human RNASET2): a) The U937 cell line do non express detectable level of endogenous RNASET2 (U937 -/-) and after addition of the crosslinker do not show any artefact (U937 -/BS3). The addition of rRNASET2 to the cells remains unexpectedly clearly visible in the cellular extract (U937 RNASET2/-). If we apply the crosslinker to the latter condition, we manage to see a shift at higher molecular weight for RNASET2 positive signals (U937 RNASET2/BS3). b) Purification of the extract over NHS-agarose beads functionalized with the anti-human RNASET2 antibody. In the elution step we cannot see any positive signal at higher molecular weight, with a limit of detection of 3ng of protein.

Development of an assay to study the role of RNASET2 in macrophages polarization

The experimental overexpression of RNASET2 in tumor xenografts has been associated with their suppression in two complementary *in vivo* systems [Acquati, 2011, 2013]. As previously mentioned the observed suppression seems to be due to the recruitment of host immune cells belonging to the monocyte/macrophages lineage; further analysis identified the infiltrate as M1 polarized macrophages [Acquati, 2013].
The role of different tumor-infiltrating macrophage types is still debated but most of the time they are associated with a faster spreading of the disease and in general with a worst outcome.
Several experiments have demonstrated that macrophages have the potential to kill tumor cells in vitro when appropriately stimulated, however, bacterial stimuli and Th1 cytokines inducing M1 type polarization are usually not present at the tumor site. Here, in contrast, differentiating macrophages are likely to encounter factors that most frequently polarize them toward the M2 phenotype, which therefore are more likely to be involved in the process of tumor progression and invasion [Mantovani, 2002].
Considering the evidence gathered so far we proposed that RNASET2 might have a role in the polarization of macrophages, hence the last part of the project was dedicated to the development of a proper assay to test the potential of RNASET2 in driving macrophages polarization. As mentioned before, tumors generally provide factors stimulating the alternative activation of macrophages towards the M2 type, therefore, along assessing whether RNASET2 is able to drive naive macrophages polarization, we were also interested in assessing a potential interference role in already polarized macrophages.
In short we planned to develop an efficient and reliable system of production and detection of M0, M1 and M2 macrophages removing any bias from endogenous RNASET2 expression.

In order to reduce the variability among human donor subjects we decided to focus our efforts on the development of an assay based on a cell line. Considering the consistent literature available, our first choice was the promyelocytic cell line THP1, which was already reported as a model for differentiation and polarization studies.
Considering our final aim (namely the study of the effect of RNASET2 in macrophages polarization) we needed to quantify the endogenous expression of RNASET2 in the THP1 cell line, which could be a disturbing variable. Indeed, the expression of the endogenous protein is quite consistent hence our first step was the development of a silenced pool of THP1 cells.
We designed a short interfering RNA (siRNA) based on the sequence of the human RNASET2 protein and cloned it in a pSico vector; the whole construct was nucleofected and, after selection, the expression of the pool was tested by WB analysis (for detail see Material and Methods). The new pool of THP1 cells have been effectively silenced for RNASET2 expression (fig 12).

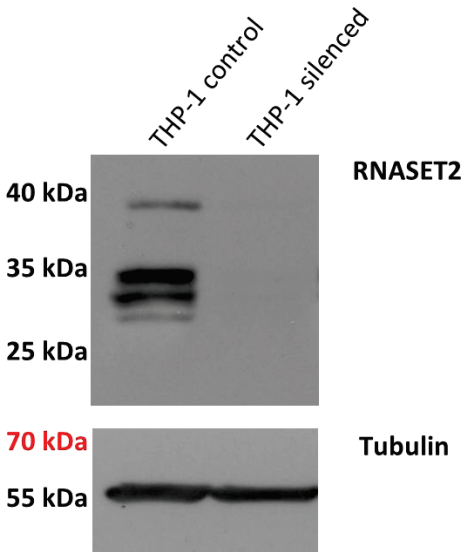

Figure 12. WB analysis of the expression of RNASET2 in THP-1 cells before and after silencing:
The upper panel show the level of expression of the endogenous RNASET2 in THP-1 cells before silencing (control) and after selection of the pool of silenced cells (silenced). As normalizer we show the expression of Tubulin.

The M1/M2 polarization is a feature macrophage-specific and the THP-1 cells, being of a promyelocytic origin, are closer to the monocyte cells; thus, as soon as we managed to obtain the silenced pool of cells, we moved to the development of a proper differentiation protocol.
To achieve this goal, we looked up the literature and identified some important guidelines: The most common approach to obtain differentiated macrophages from THP-1 cells is the use of phorbol 12-myristate 13-acetate (PMA) [Daigneault, 2010]. Generally, it is reported that the suggested working concentration to obtain macrophages from THP-1 cells is 100 ng/ml, however, some papers [Park, 2007; Maeß, 2014], suggest that this concentration might be high enough to upregulate the expressions of some genes in differentiated macrophages, which in turn could overshadow the increase in gene expression induced by other stimuli. Therefore, we decided to lower the PMA concentration to 5 ng/ml.
After some attempts, changing concentration of PMA and length of the treatment, we managed to obtain fully differentiated macrophages (M0) from silenced THP-1 cells applying 5 ng/ml PMA for 48h (fig 13).
To assess the effective differentiation, we relied on morphological observations (fig 13 a) (macrophages are attached cells, instead monocytes are floating cells) and additionally we tested the expression of a known marker of differentiation (CD68) [Genin, 2015] by qPCR (fig 13 b).

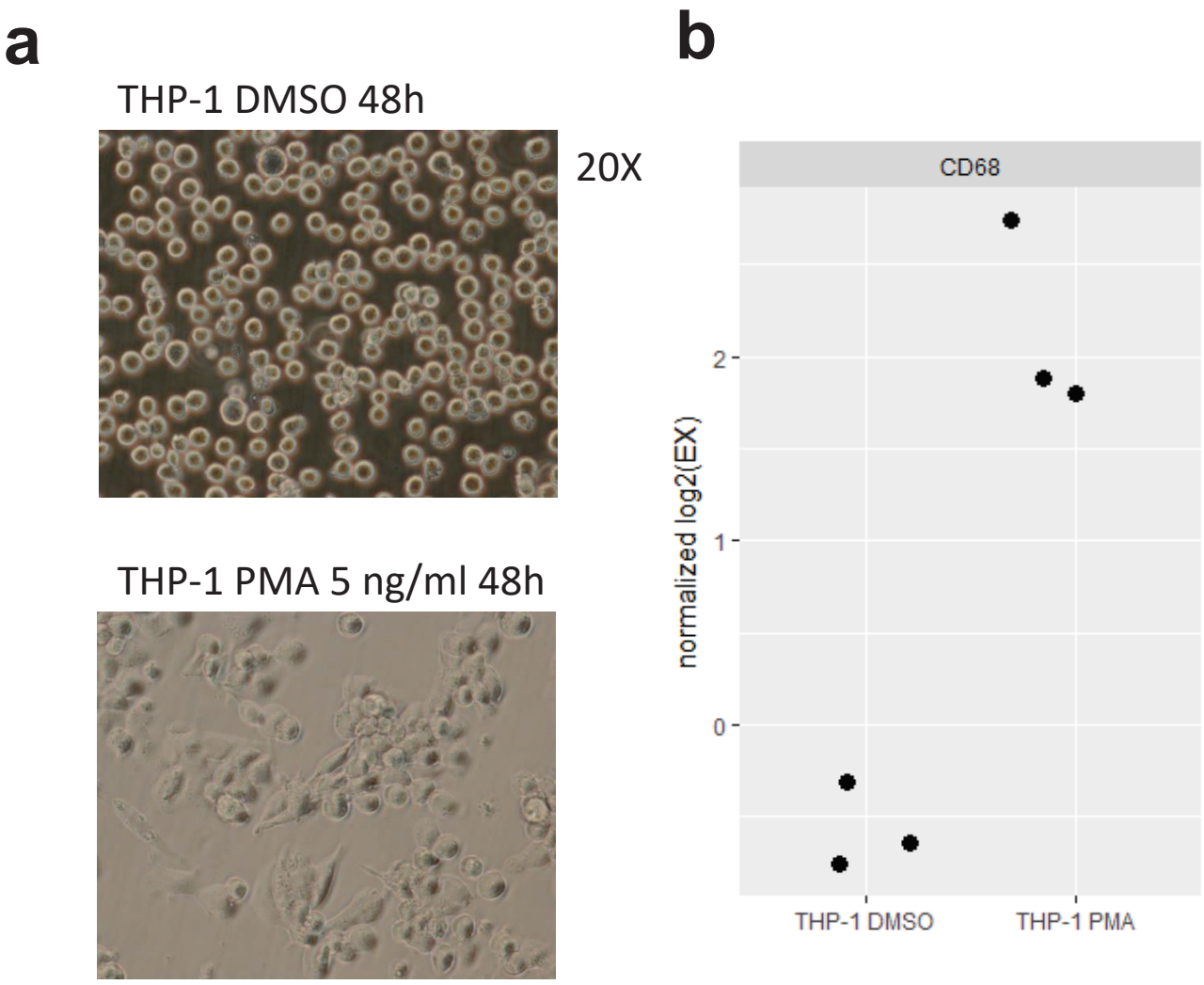

Figure 13. differentiation of silenced THP-1 cells into macrophages:
After treatment of the silenced pool of THP-1 cells with PMA 5 ng/ml for 48h the cells are clearly attached to the petri dish ((a) lower panel). To assess that the differentiation is unequivocally due to the effect of PMA, as control, we treated the cells with the vehicle of PMA (DMSO); in this case the cells do not assumed the typical flat shape and remains floating ((a) upper panel).
(b) To further confirm the effectiveness of the differentiation protocol we also tested by qPCR the expression of a well-known marker (CD68). Here is presented a strip plot showing data gathered from three independent experiments. The expression is reported as log2 of the expression level (LOD 35 cycles), using as normalizer the expression of GAPDH. The difference observed is significant with a p-value < 0.05 (t.test) and an effect size of 6.90 (Cohen's d).

The final step in the development of our functional assay entailed the setting up of a protocol for defining a proper transcriptional profile (M1 and M2).
As mentioned before the M1-M2 definition is an important issue that has to be taken into account experimentally. This basic definition actually considers different activation scenarios (different mediators can be used to produce "polarized macrophages"): the M1 type is normally produced from exposure of M0 macrophages to INF-gamma and LPS whereas the M2 is produced from exposure of M0 macrophages to IL-4. These are just two prototypic cases of a spectrum of possible profiles that cannot be easily binned into defined groups [Stout, 2004; Mantovani, 2005; Edwards, 2006; Biswas, 2010; Martinez, 2014].
To avoid misunderstanding, the recommendation is to adopt a nomenclature linked to the activation standards, i.e., M (IFN-g + LPS) and M(IL-4) instead of M1 and M2 [Murray, 2014].
In our case we decided to focus our efforts on developing a protocol to obtain the two more classical activation profiles, M (IFN-g + LPS) and M(IL-4) hence, for simplicity, from now on we will keep using the M1 and M2 definition referring to M (IFN-g + LPS) and M(IL-4) macrophages.

To obtain M1 macrophages we exposed M0 macrophages for 24h to 100 ng/ml of LPS and 20 ng/ml of INF-g and to obtain M2 macrophages 24h to 20 ng/ml of IL-4 (for detail see Material and Methods). Following this protocol, we managed to obtain differentiated macrophages (M1 and M2) without exploring other solutions (fig 14).

The association of a sample to a specific polarization profile (M1 or M2) cannot rely on a single marker therefore, we chose a small panel of known marker of polarization tested by qPCR (fig 14 a).
TNF, CXCL10, CCL19 are reported as marker of M1 polarization, meaning that the expression of those genes is expected to be higher in M1 compared to M2 [Maeß, 2014].
CCL22, MRC1, MSR1 are reported as marker of M2 polarization, meaning that the expression of those genes is expected to be higher in M2 compared to M1 [Martinez, 2006; Medina, 2011]. It is clearly visible that all the genes listed above behaved as expected (fig 14 a).

Considering the final step of the assay (namely to assess whether RNASET2 is able to drive/interfere with macrophages polarization), as the last control, we decided to check whether our macrophage samples were able to "transit" form their assigned profile. In other terms we wanted to develop a control that could tell us whether the macrophages still retained the plasticity to change their profile according to external stimuli.
Definitely the M0 macrophages produced were as expected, in fact, when exposed to known polarizing stimuli, they assumed the expected polarization profile (fig 14 a, b). The next main question concerned M1 and M2 macrophages; were our M1cells still able to change their profile if exposed to known M2 stimuli and what about the M2 cells exposed to known M1?
To answer this question, we decided to use as a control M0 cells exposed to both the M1 and M2 stimuli (these samples were called MX). The result (fig 14 a, b) showed that the profile obtained was neither M1 nor M2, suggesting that the cells prepared with our system still retained the characteristic/desired plasticity to properly respond to external signals.

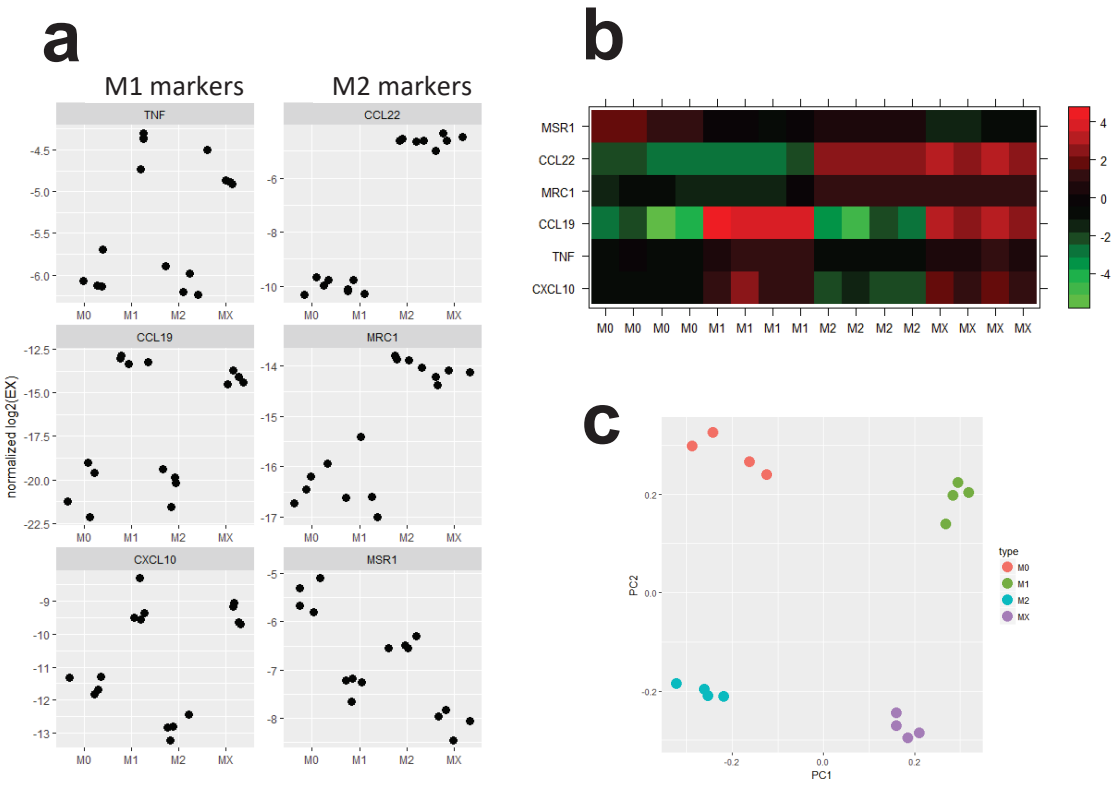

Figure 14. analysis of the expression of known marker of polarization:
We tested the expression of known marker of polarization over the end-product of our polarization protocol. In the strip plot (a) is shown, as expected, that each cell types (M1 vs. M2) correctly overexpress the specific markers.
MX is a control sample derived from the exposure of M0 to M1 and M2 stimuli; the purpose of this control is to verify whether either M1 or M2 induced macrophages (produced with our system) are still able to react to contradictory stimuli. As clearly shown in the heatmap (b) MX are not associable to any phenotype, meaning that both M1 and M2 induced profile can be still influenced by external stimuli.
Finally, the PCA (c) recapitulate both the strip plot and the heatmap. Each sample is clearly separated from the others; the system developed might be ready to test the role of RNASET2 (or any other compound) in macrophages polarization.
In (a) are shown data gathered from four independent experiments. The expression is reported as log2 of the expression level (LOD 35 cycles), using as normalizer the expression of GAPDH. The difference observed between the expression level in M1 and M2 is significant with a p-value < 0.05 for all the markers (MANOVA followed by ANOVA over every variable and TukeyHSD test) the effect size estimated is grater that 0.9 for each variable (Ƞ^2).
To produce (b) expression data were further normalized by standardization (z-scores).

Considering all the data gathered so far we think that this system might be used as an assay to assess the role of RNASET2 (or any other compound) in macrophages polarization.

DISCUSSION

The *RNASET2* gene encodes for the only human secreted acid ribonuclease of the T2 family. This gene maps in 6q27, a region that is consistently found rearranged in many solid and hematological tumors [Acquati, 2005]. Experimental data gathered in our laboratory have demonstrated the role of RNASET2 as a tumor suppressor gene which is endowed with several functions including chemotactic and possibly activating activities toward the monocyte/macrophage population [Acquati, 2011]. In a mouse xenograft model, we have recently reported that inoculation of human ovarian cancer-derived cells forced to overexpress RNASET2 led to the development of small, growth-suppressed tumors, characterized by a strong infiltrate of host-derived innate immunity cells, which have been identified as mainly M1 polarized macrophages. By contrast, control cells not expressing RNASET2, developed large, fast-growing tumors with no sign of macrophage infiltration.
Further investigations proved that recombinant RNASET2 (produced in either baculovirus or *Pichia pastoris* expression system) displayed a marked chemotactic activity *in vitro,* most likely dependent on a subfamily of G-protein Coupled Receptors associated with inhibitory G protein [Acquati, 2013].
Taken together, these results led us to suggest that RNASET2-mediated *in vivo* tumor suppression is a non-cell-autonomous process which result in the recruitment of macrophages into the tumor mass.
Based on such evidences, we decided to further investigate the relation between RNASET2 and cells belonging to the monocyte-macrophages lineage.

Most of the experiments we planned to carry out involved the use of purified recombinant human RNASET2, hence, the first step of the project was the development of a reliable supply system.
Two different sources of production and purification of human RNASET2 protein were already available in our lab (P. pastoris and BEVS) [Campomenosi, 2011], however, a full exploitation of these reagents was precluded by several limitations inherent to both systems. The end-product was highly heterogeneous due to high molecular weight species co-eluting with the RNASET2 molecule. Moreover, the purification steps were not optimized and a significant amount of recombinant protein was lost in the in both flow-through and wash fractions during affinity purification. Finally, the eluted protein displayed a significant LPS contamination, which clearly precluded its use in functional assays involving cells from the monocyte/macrophage lineage that likely represent the most relevant target of the RNASET2 protein *in vivo*.
To overcome these limitation, we decided to focus our efforts on improving the *P. pastoris* expression system, which was more cost-effective and easier to handle in term of available facilities.
The previously described system [Campomenosi, 2011] made use of the X33 Pichia *Pastoris* strain, transformed with a plasmid (pPICZ alpha A) coding for the human wild type RNASET2 protein tagged with a C-terminal 6XHis tag (wt_RNASET2-His). The purification process relied on an IMAC followed by a SEC as polishing step.
Our first attempt to improve the system was to explore new purification conditions. By this approach, we manage to assess that the polishing step with SEC should be replaced with an IEX, but still a considerable amount of protein was lost in the FT. To solve the problem, we added another 6XHis tag to the construct coding for the human RNASET2 and managed to significantly improve the recovery of the input protein. Finally, we confirmed the successful yield increase of the new recombinant protein by performing a zymogram.
Considering the downstream applications of the purified human RNASET2, contamination of the preparation by metals (especially Ni, Cd, Zn) and endotoxin are important factor to control in order to properly assess a relationship between a specific treatment (in our case the addition of recombinant

human RNASET2) and immune cell response. Applying the proper care in the preparation of the buffers and the handling of the sample we manage to achieve a low endotoxin content and an undetectable level of contamination by metals (Ni, Cd, Zn).

P. pastoris provide all the features of eukaryotic protein synthesis, making it a better expression system compared to bacteria as host for recombinant eukaryotic proteins. The recombinant human RNASET2 produced with this new system thus meets the minimum requirements to perform reliable studies with human macrophages. However, despite having the same sequence of the human protein, the recombinant RNASET2 expressed in this system is slightly different from the RNASET2 produced by human protein produced by human cells, and a main concern is represented by the pattern of protein glycosylation. *Saccharomyces cerevisiae* (another widely used host for recombinant protein production) and *Pichia pastoris* mainly display N-linked glycosylation of the high-mannose type, but the length of the oligosaccharide chains post-translationally added to *Pichia* proteins (average 8–14 mannose residues per side chain) is much shorter than the one observed in Saccharomyces cerevisiae (50– 150 mannose residues) [Grinna, 1989; Tschopp, 1987b], whose proteins are known to be particularly unsuitable for therapeutic use due to the strong antigenic response. In this context, the *Pichia pastoris* glycosylation pattern more closely resembles the pattern observed in higher eukaryotes [Cregg, 1993].
From these premises and as a possible future research option, we evaluated two ways to further improve the experimental system.
The first idea is to replace *P. pastoris* with a human cell line in order to produce a "fully human" protein. We carried out a pilot experiment in the Hey3Met2 cell line (a clone derived from the ovarian carcinoma cell line HEY4) but we could not achieve adequate level of expression. A future option could be to turn to the PER-C6 cell line (from human retinal tissue), that has been reported to reach 500 mg/l of recombinant proteins [Jones, 2003].
An alternative approach is to perform a native deglycosylation of the batch of protein currently available. As a pilot experiment we tested different enzymes and identified Endoglycosidase H (EndoH) as a good candidate. EndoH is a recombinant glycosidase which cleaves within the chitobiose core of high mannose and some hybrid oligosaccharides from N-linked glycoproteins [Koide, 1974] Since it does not need access to the protein backbone to exploit its activity, it represents a suitable enzyme for native deglycosylation assays. We are currently planning to perform a Mass Spectrometry (MS) analysis of the end-product from EndoH digestion of recombinant RNASET2 to assess the level of deglycosylation reached with our protocol. The native deglycosylation might be useful not only as an alternative to the PER-C6 approach, but could also be applied to the "fully human" protein to further investigate the role of glycosylation in monocyte recruitment and macrophages polarization.

As previously mentioned, several studies have reported the consistent tumor suppressive role for several members of the T2 RNase protein family [Smirnoff, 2006; Schwartz, 2007] and the recruitment of immune cells seems to be involved in this suppression [Acquati, 2011, 2013].
In order to improve our knowledge of these functional features of T2 RNases and at the same time to evaluate their evolutionary conservation, we tested the role of human recombinant RNASET2 in the activation and recruitment of immune cells by injecting recombinant human RNASET2 in the body wall of *Hirudo verbena* a useful model system for our purposes.

After rRNASET2 injection, a significant increase in the production of collagen fibrils and a consequent remodeling of the muscle layers was observed. The resulting massive production of connective tissues is then used as a scaffold for immune cells migration and for proper orientation of growth of new vessels [de Eguileor, 2004; Tettamanti, 2004]. In this regard, it is worth noting that human RNASET2 was recently

shown to affect both the cytoskeletal organization and the migratory pattern of ovarian cancer cell lines [Lualdi, 2015].

Injection of human recombinant RNASET2 was also shown to induce a massive migration of cells belonging to the macrophages lineage (characterized as HmAIF-1+ and CD68+ cells) within 24 h, coupled to the formation of new blood vessels.
The observed inflammatory response was specifically dependent of recombinant RNASET2 injection, since infiltrating macrophages and neo-vessel formation were not observed following injection of either PBS or rRNASET2 protein that was pre-incubated with a neutralizing anti-RNASET2 antibody.
Taken together, these data strongly suggest that rRNASET2 injection in leeches induces a marked inflammatory response characterized by macrophage recruitment.

Unexpectedly we observed a positive signal both by IF and western blot using the anti-human RNASET2 antibody with leech cells. This result led us to suppose the existence of a putative endogenous and homologous T2 ribonuclease(s) in Hirudo.
In this regard, the observation that recombinant RNASET2-mediated infiltration of leech macrophages is associated with a marked increase in the expression of putative endogenous RNASET2 by the same macrophage cells suggests that such an endogenous RNASET2 increase might further contribute in the recruitment and accumulation of more macrophages in the stimulated body region. Although the occurrence of such RNASET2-based positive feedback mechanisms on target infiltrating cells could be speculative, our results though are in agreement with data previously reported in other organisms. Indeed, proteins belonging to the Rh/T2/S ribonuclease family (including RNASE T2) are known to be actively secreted from cells belonging to different phyla ranging from yeast to human and once in the extracellular medium they exert their actions [Luhtala, 2010; Acquati, 2011, 2013].

Taken together, these observations are in keeping with the role of RNASET2 as an inducer of a consistent inflammatory response. Of note, RNASET2-mediated activation and recruitment of macrophages seems to represent an evolutionarily conserved process, since in this work we were able to recapitulate it also in an invertebrate experimental model. In keeping with this hypothesis, recent work on the trematode *Schistosoma mansoni* has demonstrated a role for a T2 RNase protein encoded by the parasite's genome (omega-1) in the modulation of the innate immune response in infected hosts [Ferguson, 2015].
We investigated the marked RNASET2-mediated infiltration of leech macrophages observed *in vivo* by further assessing the chemotactic activity of recombinant RNASET2, using a consolidated experimental approach based on injection of MG biopolymers supplemented with soluble factors in the leech body wall. Histological and immunocytochemical assays on explanted rRNASET2- supplemented MG pellets showed a massive infiltration of host cells that stained positive for CD68 or HmAIF-1 markers, thus providing further evidence in support of the chemotactic activity of RNASET2 on macrophage cells.

Finally, we show that injection of LPS in the body wall of leech not only causes a massive migration of CD68+/ HmAIF-1+macrophages as previously described [de Eguileor, 1999; Schorn, 2015a,b] but also induces a strongly increased expression of endogenous RNASET2 in these migrating macrophages, as assessed by both immunohistochemical and western blot analysis. It is well known that, in response to infections, leech macrophages produce antimicrobial proteins and peptides that specifically disrupt several components of Gram-positive bacterial cell walls [Schikorski, 2008; Hildebrandt, 2011]. The observed increase of homologous RNASET2 expression by leech macrophages could therefore be directly correlated to its putative ability to act as a stress response protein by priming host macrophages for mounting an anti-bacterial response. In this regard, it is worth noting that a marked stress response role for human RNASET2 has also been recently reported in human cancer cells [Lualdi, 2015],

again supporting the occurrence of an ancient and evolutionarily conserved role for this gene. Moreover, since some ribonucleases have been described to display a marked antimicrobial activity [Boix, 2012], a direct anti-bacterial role for the RNASET2 enzyme cannot be ruled out, although this hypothesis remains largely speculative at present.
Thus the data reported provide compelling evidence in support of a role for RNASET2 as a key component of the innate immune system, not only in vertebrates but also in invertebrates. If confirmed by further investigations, this scenario would suggest a complex, pleiotropic role for RNASET2 in orchestrating an evolutionarily conserved inflammatory response, mainly based on macrophage recruitment and activation coupled to a massive extracellular remodeling.

Taken together, the data gathered in our lab in several *in vitro* and *in vivo* experimental systems strongly suggest the occurrence of an RNASET2-based intercellular cross-talk, whose molecular mechanisms are nevertheless largely unknown.
As a first step in the logical sequence of events culminating in the above mentioned RNASET2 biological activities, we hypothesized the occurrence of a putative receptor for RNASET2.
The common idea behind all our approaches was to covalently link RNASET2 (either the endogenous protein or the human recombinant protein) to any interactor and, after purification of the complex, to perform a MS analysis to characterize the interactants.
As a first approach, we carried out chemical modification of purified recombinant RNASET2 with different compounds (SDA, LC-SDA, Sulfo SDA, Sulfo LC-SDA) in order to add a diazirine ring to all primary ammines of the target protein. The resulting modified RNASET2 protein could then, in principle, be crosslinked to all electron donors available following UV light activation. The modified protein was then incubated with RNASET2-silenced OVCAR3 cells and analyzed by western blot following UV exposure. Despite several attempts with this approach, we could not observe any shift in the molecular weight of RNASET2.
As a second approach, parental OVCAR3 cells expressing RNASET2 were cultured in a medium containing photo-reactive amino acids, making the modified proteins prone to UV-crosslinking but, even with this approach, we failed to see any detectable shift in the molecular weight of RNASET2.
Considering that most of the result obtained show evidence of a tropism of RNASET2 for cells belonging to the monocyte/macrophage lineage, with our last approach tested a promyelocytic cell line. We exposed the U937 cells preincubated with rRNASET2 to a chemical crosslinkers (BS3) able to covalently link two or more proteins in close proximity. By this approach we managed to see a shift in the molecular weight of the RNASET2, but unfortunately in the next step we couldn't purify any detectable complex.

There are many reasons that could explain our failures:

- An RNASET2 receptor might not exist although in our last attempt we cannot definitively exclude its existence.
- The putative RNASET2 receptor might expressed at very low levels, hence the WB technique might not be sensitive enough to detect it. To solve this problem, we could scale up the system or work with membrane enriched samples.
- The covalent modification produced by the chemical crosslinkers might produce a complex that is no more recognizable by the antibody used in the WB or purification step. A possible solution in order to overcome this problem consists in performing a classical IP over a membrane enriched extract and, to further reduce the detection problems, proceed with MS analysis over the whole SDS-gel lane.
- Finally, recent experiments conducted by our collaborators provide evidence that RNASET2 might be present inside extracellular vesicles (exosomes). This result opens new opportunities of research and might change our prospective about the mechanism behind RNASET2 sensing and trafficking.

Considering that TAMs are usually forced by the tumor cells to acquire an M2-polarized pro-tumorigenic phenotype, a key finding of our research group is that tumor xenografts that are suppressed in their growth following RNASET2 overexpression display a strong infiltration of M1-polarized macrophages [Acquati, 2011, 2013], which are known to show anti-tumorigenic properties. Therefore, the last part of this PhD program was dedicated to investigate the molecular/cellular bases of the interaction between RNASET2 and immune cells, in particular to describe a possible involvement of this protein in driving macrophages polarization.
The main idea was to develop a system to reliably produce M0, M1 and M2 macrophages that could then be used to test the effect of RNASET2 looking at their transcriptional profile.
To this end, we chose a well-known cellular model (THP-1 cell line) and, in order to remove any bias from future analysis, we selected a pool of cells silenced for the expression of RNASET2.
THP-1 is a promyelocytic cell line therefore in order to effectively produce polarized cells we needed to differentiate it into macrophages. Using the guidelines found in the literature we managed, by treating THP-1 cells with PMA 5 ng/ml for 48 h, to produce M0 macrophages.
Subsequently, we developed a protocol to effectively drive naive macrophages to either M1 or M2 phenotype. We followed the suggested guidelines and assessed the efficacy of our system by testing a small panel of known marker of polarization (TNF, CXCL10, CCL19 for M1 polarization and CCL22, MRC1, MSR1 for M2 polarization).
Considering the final aim of the developed assay, we tested whether our macrophages, especially M1 and M2, still retained the plasticity to change their profile according to external stimuli. M0 cells were exposed to both M1 and M2 stimuli; the resulting profile was neither M1 nor M2, suggesting that the cells prepared with our system still retained the characteristic/desired plasticity to properly respond to external signals.
The data gathered so far support the idea that the system developed might be useful to study the involvement of RNASET2 in macrophages polarization.

To summarize, during these three years of my PhD program I was involved in many different parts of a project aimed at deepen our understanding of the mechanism underlying RNASET2 tumor suppression. Although I wasn't able to identify any putative receptor for RNASET2 experimental evidence suggests the existence of a molecular mechanism involved in the “sensing” of the RNASET2 protein. Further studies are clearly needed in order to clarify this issue and the recent finding of RNASET2-containing exosomes is a promising avenue of investigation.

The data collected in *Hirudo* strengthen our hypothesis of a close relationship between Immune cells (in particular cells belonging to monocyte/macrophages lineage) and RNASET2 but, more importantly these results open new research opportunities to study the involvement of T2 ribonucleases in inflammation.
From a strictly technical point of view, I was able to improve the system of production and purification of the recombinant human protein, making it possible the use of RNASET2 in conditions previously inaccessible (interaction with immune cells/injection in organism).
To conclude I contributed to laid the bases for future studies aiming at dissecting the involvement of RNASET2 in macrophages polarization and I did it by developing a simple assay that might test the "polarizing potential" of RNASET2 (but potentially of any compound).

Concluding remarks

In January 2016, through the help of my tutor, Prof. Roberto Taramelli, I had the opportunity to move to the USA in the laboratory of Prof. Sui Huang at the Institute for Systems Biology, Seattle WA. Here, for 10 months, I gained familiarity with the exploitation of computational tools to answer biological questions and I have also been exposed to the emerging field of computational/systems biology.
The central role of genetic mutations as the driving force for tumorigenesis and tumor progression is challenged by the increasing recognition of cell population heterogeneity and plasticity, which can generate different phenotypes from a single genome [Zhou, 2016]. The main research interest of Prof Hung's lab is to address the origin(s) of heterogeneity and in particular what are its consequences for tumor development. During this period, I have been involved in and contributed to three different projects:

The first project was focused on the understanding of the role of adaptation in cancer drug resistance.
When cancer cells fail to respond to chemotherapy regimes the usual explanation focuses on the presence of inherently resistant cells produced by random mutations, which are then selected for.
However, within the framework of the population heterogeneity and cell plasticity, the resistance phenotype can be acquired exploiting physiological cellular programs [Chang, 2008].
Among them one that is gaining much attention is the cellular stress response adaptation following chemotherapy or irradiation. The basic hypothesis is that the treatments are indeed inducing the tumor cell to enter a stress response state which in turn protects them from the noxious agent [Huang, 2009, 2010].
I used the leukemic HL60 cell line as the cancer model and I studied the response of the cells to Vincristine treatment.
In order to assess how the emerging phenotype (the drug resistance) was induced following treatment, we analyzed a population of treated cells at the single cell level. To address this issue, I learnt a new technique called single cell qPCR which allows to quantify the gene expression profile from a single cell. Furthermore, the single cell resolution allows to study the occurrence of the rare and underrepresented cells within a given population.
Preliminary results show the emergence of a subgroups of cells, within the main population, characterized by the expression of stemness markers and further analyses are required to demonstrate whether these cells are associated with the emergence of drug resistance.

The second project was aimed at the development of an assay to estimate the proliferation rate of a single cell culture in a longitudinal study; in particular, I developed a pipeline that allows to measure the area occupied by cell in every well of a 384-wells plate for each defined time point.
Previous observations using an *in vivo* model suggested that the per capita growth rate of the cell is dependent on the cell density (Allee effect) [unpublished data]. Within this conceptual frame, we were interested in collecting data that could support a new model to describe the cell proliferation also *in vitro*.
In the first two months of work I developed the pipeline for the analysis as follows:

- I have written the script to control the acquisition of a grid of images and iterate the process for every desired well in a 384-wells plate.

- I have also written a script in ImageJ that can stitch together the grid for each well and produce a single image and another script that measures the cell in an image. The “area occupied by the cell” is the variable analyzed in order to test our model.

As a first experiment I measured the growth rate of different cultures starting with different cell numbers: 1 cell, 4 cells, 10 cells (80 wells per each condition). The result shows that cells plated at the density of 10 cells have a more consistent behavior and a per capita growth rate higher than cells plated at lower initial density (4 and 1 respectively). We are currently building a mathematical model that could fit and explain the gathered data.

The third project I contributed to was focused on the analysis of the dysregulation of the chemokine-cytokine and cognate receptors expression in different cancer tissues. We used a database of 2536 know chemo-cytokines/cognate receptors interactions and the data were collected from The Cancer Genome Atlas (TCGA) database. The basic idea was to assess whether and how the communication provided by the ligand receptor interaction is changed in cancer compared to normal tissues.
We focused on the pairwise analysis of the correlation of the expression of the ligand (chemo-cytokine) versus its receptor.
The main observation is that in cancer tissues there’s a general loss of correlation, either positive or negative with respect to normal tissues. This finding might depict cancer as a “less communicative” entity, which is not able to react properly to certain stimuli, especially from the ligand receptor interactions we decided to assess.
Since the TCGA data are retrieved from bulk RNA samples, it is not possible to define the exact composition in term of cells type; the only information available in this sense is the percentage of infiltrating immune cells. Knowing that most of the ligand receptor interaction are mainly mediated by immune cells we checked whether our previous finding is a genuine feature of cancer cells, or a side-effect due to a different percentage of infiltrating immune cells.
Interestingly, clustering the samples by percentage of infiltrating immune cells do not affect the overall distribution of the correlation; this allow us to infer that the observation of a different distribution of correlation is a true feature of the cancer cells (or at least is not driven by the percentage of infiltrating immune cells).
An interesting question we tried to investigate is whether it is possible to define (or at least suggest) “who talks with who” in term of different cell type. As mentioned before the TCGA data are a large source of information but these data are averages of the expression of all the different cells that make up a tissue; this means that is not possible the associate the value of expression to any specific cell type. Therefore, in order to address this question, we used single cell RNAseq data from melanoma samples (19 different patients) recently published [Tirosh, 2016].
Single cell RNAseq data allow to quantify the expression of different genes from just one cell. Having a single cell level resolution is critical from certain viewpoints, especially if the goal is to understand the heterogeneity of a system or to identify very rare subpopulations.
In our case single cell data were useful because we were able to measure the expression of ligands and receptors from virtually pure tissues inside the same sample.
As criteria for the present analysis we assumed that the cells (among all the others inside the sample) with a significant higher expression of a specific ligand are defined “major broadcasters” (for that specific ligand), and the cells with a significant higher expression of a receptor are defined “major receivers”. Our

hypothesis is that if we assume a communication between cells, then is more likely that the major broadcasters would “talk” to the major receivers.
Given that assumption and focusing on interactions from cancer cells or towards them, we were able to define a higher cross-talk between CAF or endothelial cells (rather than immune cells) with cancer cells.

This result, although preliminary, is promising and could be exploited in more targeted experiments in order to better understand the crosstalk between cancer cells and the single cells comprising the microenvironmental populations.

REFERENCES

[**Acquati, 2001**] Acquati F, Morelli C, Cinquetti R, Bianchi MG, Porrini D, Varesco L, Gismondi V, Rocchetti R, Talevi S, Possati L, Magnanini C, Taramelli R. Cloning and characterization of a senescence inducing and class II tumor suppressor gene in ovarian carcinoma at chromosome region 6q27. Oncogene. 2001 Feb 22;20(8):980.

[**Acquati, 2005**] Acquati F, Possati L, Ferrante L, Campomenosi P, Talevi S, Bardelli S, Margiotta C, Russo A, Bortoletto E, Rocchetti R, Calza R, Taramelli R. Tumor and metastasis suppression by the human RNASET2 gene. International journal of oncology. 2005 May 1;26(5):1159-68.

[**Acquati, 2011**] Acquati F, Bertilaccio S, Grimaldi A, Monti L, Cinquetti R, Bonetti P, Lualdi M, Vidalino L, Fabbri M, Sacco MG, van Rooijen N, Taramelli R. Microenvironmental control of malignancy exerted by RNASET2, a widely conserved extracellular RNase. Proceedings of the National Academy of Sciences. 2011 Jan 18;108(3):1104-9.

[**Acquati, 2013**] Acquati F, Lualdi M, Bertilaccio S, Monti L, Turconi G, Fabbri M, Grimaldi A, Anselmo A, Inforzato A, Collotta A, Cimetti L, Taramelli R. Loss of function of Ribonuclease T2, an ancient and phylogenetically conserved RNase, plays a crucial role in ovarian tumorigenesis. Proceedings of the National Academy of Sciences. 2013 May 14;110(20):8140-5.

[**Allavena, 2000**] Allavena P, Sica A, Vecchi A, Locati M, Sozzani S, Mantovani A. The chemokine receptor switch paradigm and dendritic cell migration: its significance in tumor tissues. Immunological reviews. 2000 Oct 1;177(1):141-9.

[**Balkwill, 2001**] Balkwill F, Mantovani A. Inflammation and cancer: back to Virchow?. The lancet. 2001 Feb 17;357(9255):539-45.

[**Bhowmick, 2004**] Bhowmick NA, Neilson EG, Moses HL. Stromal fibroblasts in cancer initiation and progression. Nature. 2004 Nov 18;432(7015):332-7.

[**Bissell, 2001**] Bissell MJ, Radisky D. Putting tumours in context. Nature Reviews Cancer. 2001 Oct 1;1(1):46-54.

[**Biswas, 2010**] Biswas SK, Mantovani A. Macrophage plasticity and interaction with lymphocyte subsets: cancer as a paradigm. Nature immunology. 2010 Oct 1;11(10):889-96.

[**Boix, 2012**] Boix E, Salazar VA, Torrent M, Pulido D, Nogués M, Moussaoui M. Structural determinants of the eosinophil cationic protein antimicrobial activity. Biological Chemistry. 2012 Aug 8; 393(8): 801–815.

[**Breading, 2006**] Beadling C, Slifka MK. Regulation of innate and adaptive immune responses by the related cytokines IL-12, IL-23, and IL-27. Archivum immunologiae et therapiae experimentalis. 2006 Feb 1;54(1):15-24.

[**Campomenosi, 2006**] Campomenosi P, Salis S, Lindqvist C, Mariani D, Nordström T, Acquati F, Taramelli R. Characterization of RNASET2, the first human member of the Rh/T2/S family of glycoproteins. Archives of biochemistry and biophysics. 2006 May 15;449(1):17-26.

[**Campomenosi, 2011**] Campomenosi P, Cinquetti R, Tallarita E, Lindqvist C, Raimondi I, Grassi P, Näsman J, Dell A, Haslam SM, Taramelli R, Acquati F. Comparison of the baculovirus-insect cell and Pichia pastoris heterologous systems for the expression of the human tumor suppressor protein RNASET2. Biotechnology and applied biochemistry. 2011 Jan 1;58(1):39-49.

[**Chang, 2008**] Chang HH, Hemberg M, Barahona M, Ingber DE, Huang S. Transcriptome-wide noise controls lineage choice in mammalian progenitor cells. Nature. 2008 May 22;453(7194):544-7.

[**Clark, 1991**] Clark WH. Tumour progression and the nature of cancer. British journal of cancer. 1991 Oct;64(4):631.

[**Colitti, 1998**] Colitti CV, Rodabaugh KJ, Welch WR, Berkowitz RS, Mok SC. A novel 4 cM minimal deletion unit on chromosome 6q25. 1-q25. 2 associated with high grade invasive epithelial ovarian carcinomas. Oncogene. 1998 Feb;16(4):555-9.

[**Coussens, 2000**] Coussens LM, Tinkle CL, Hanahan D, Werb Z. MMP-9 supplied by bone marrow–derived cells contributes to skin carcinogenesis. Cell. 2000 Oct 27;103(3):481-90.

[**Cregg, 1993**] Cregg JM, Vedvick TS, Raschke WC. Recent advances in the expression of foreign genes in Pichia pastoris. Nature Biotechnology. 1993 Aug 1;11(8):905-10.

[**D'Alessio, 1997**] D'Alessio G. New and cryptic biological messages from RNases. Trends in cell biology. 1993 Apr 1;3(4):106-9.

[**Daigneault, 2010**] Daigneault M, Preston JA, Marriott HM, Whyte MK, Dockrell DH. The identification of markers of macrophage differentiation in PMA-stimulated THP-1 cells and monocyte-derived macrophages. PloS one. 2010 Jan 13;5(1):e8668.

[**de Eguileor, 1999**] De Eguileor M, Grimaldi A, Boselli A, Tettamanti G, Lurati S, Valvassori R, Lanzavecchia G. Possible roles of extracellular matrix and cytoskeleton in leech body wall muscles. Journal of microscopy. 1999 Oct;196(1):6-18.

[**de Eguileor, 2001**] De Eguileor M, Grimaldi A, Tettamanti G, Ferrarese R, Congiu T, Protasoni M, Perletti G, Valvassori R, Lanzavecchia G. Hirudo medicinalis: a new model for testing activators and inhibitors of angiogenesis. Angiogenesis. 2001 Dec 1;4(4):299-312.

[**de Eguileor, 2003**] Eguileor M, Tettamanti G, Grimaldi A, Congiu T, Ferrarese R, Perletti G, Valvassori R, Cooper EL, Lanzavecchia G. Leeches: immune response, angiogenesis and biomedical applications. Current pharmaceutical design. 2003 Jan 1;9(2):133-47.

[**de Eguileor, 2004**] Eguileor MD, Tettamanti G, Grimaldi A, Perletti G, Congiu T, Rinaldi L, Valvassori R. Hirudo medicinalis: avascular tissues for clear-cut angiogenesis studies?. Current pharmaceutical design. 2004 Jun 1;10(16):1979-88.

[**Dinapoli, 1996**] Dinapoli MR, Calderon CL, Lopez DM. The altered tumoricidal capacity of macrophages isolated from tumor-bearing mice is related to reduce expression of the inducible nitric oxide synthase gene. Journal of Experimental Medicine. 1996 Apr 1;183(4):1323-9.

[**Drago, 2014**] Drago F, Sautière PE, Marrec-Croq F, Accorsi A, Camp C, Salzet M, Lefebvre C, Vizioli J. Microglia of medicinal leech (Hirudo medicinalis) express a specific activation marker homologous to vertebrate ionized calcium-binding adapter molecule 1 (Iba1/alias aif-1). Developmental neurobiology. 2014 Oct 1;74(10):987-1001.

[**Egeblad, 2010**] Egeblad M, Nakasone ES, Werb Z. Tumors as organs: complex tissues that interface with the entire organism. Developmental cell. 2010 Jun 15;18(6):884-901.

[**Evan, 1998**] Evan G, Littlewood T. A matter of life and cell death. Science. 1998 Aug 28;281(5381):1317-22.

[**Ferguson, 2015**] Ferguson BJ, Newland SA, Gibbs SE, Tourlomousis P, dos Santos PF, Patel MN, Hall SW, Walczak H, Schramm G, Haas H, Dunne DW. The Schistosoma mansoni T2 ribonuclease omega-1 modulates inflammasome-dependent IL-1β secretion in macrophages. International journal for parasitology. 2015 Nov 30;45(13):809-13.

[**Gatenby, 2014**] Gatenby RA, Cunningham JJ, Brown JS. Evolutionary triage governs fitness in driver and passenger mutations and suggests targeting never mutations. Nature communications. 2014;5:5499.

[**Genin, 2015**] Genin M, Clement F, Fattaccioli A, Raes M, Michiels C. M1 and M2 macrophages derived from THP-1 cells differentially modulate the response of cancer cells to etoposide. BMC cancer. 2015 Aug 8;15(1):577.

[**Gietz, 1995**] Gietz RD, Schiestl RH, Willems AR, Woods RA. Studies on the transformation of intact yeast cells by the LiAc/ss-DNA/PEG procedure. Yeast. 1995 Apr 15;11(4):355-60.

[**Girardello, 2015a**] Girardello R, Drago F, de Eguileor M, Valvassori R, Vizioli J, Tettamanti G, Grimaldi A. Cytokine impregnated biomatrix: a new tool to study multi-wall carbon nanotubes effects on invertebrate immune cells. Journal of Nanomedicine & Nanotechnology. 2015 Sep 1;6(5):1.

[**Girardello, 2015b**] Girardello R, Tasselli S, Baranzini N, Valvassori R, de Eguileor M, Grimaldi A. Effects of carbon nanotube environmental dispersion on an aquatic invertebrate, Hirudo medicinalis. PloS one. 2015 Dec 4;10(12):e0144361.

[**Grimaldi, 2004**] Grimaldi A, Tettamanti G, Rinaldi L, Perletti G, Valvassori R, De Eguileor M. Role of cathepsin B in leech wound healing. ISJ. 2004;1:38-46.

[**Grimaldi, 2006**] Grimaldi A, Tettamanti G, Perletti G, Valvassori R, de Eguileor M. Hematopoietic cell formation in leech wound healing. Current pharmaceutical design. 2006 Aug 1;12(24):3033-41.

[**Grimaldi, 2008**] Grimaldi A, Bianchi C, Greco G, Tettamanti G, Noonan DM, Valvassori R, de Eguileor M. In vivo isolation and characterization of stem cells with diverse phenotypes using growth factor impregnated biomatrices. PloS one. 2008 Apr 2;3(4):e1910.

[**Grimaldi, 2009**] Grimaldi A, Banfi S, Gerosa L, Tettamanti G, Noonan DM, Valvassori R, de Eguileor M. Identification, isolation and expansion of myoendothelial cells involved in leech muscle regeneration. PloS one. 2009 Oct 30;4(10):e7652.

[**Grimaldi, 2011**] Grimaldi A, Banfi S, Vizioli J, Tettamanti G, Noonan DM, de Eguileor M. Cytokine Loaded Biopolymers as a Novel Strategy to Study Stem Cells during Wound-Healing Processes. Macromolecular bioscience. 2011 Aug 11;11(8):1008-19.

[**Grinna, 1989**] Grinna LS, Tschopp JF. Size distribution and general structural features of N-linked oligosaccharides from the methylotrophic yeast, Pichia pastoris. Yeast. 1989 Mar 1;5(2):107-15.

[**Hamza, 2010**] Hamza T, Barnett JB, Li B. Interleukin 12 a key immunoregulatory cytokine in infection applications. International journal of molecular sciences. 2010 Feb 26;11(3):789-806.

[**Hanahan, 1996**] Hanahan D, Folkman J. Patterns and emerging mechanisms of the angiogenic switch during tumorigenesis. cell. 1996 Aug 9;86(3):353-64.

[**Hanahan, 2000**] Hanahan D, Weinberg RA. The hallmarks of cancer. cell. 2000 Jan 7;100(1):57-70.

[**Hanahan, 2011**] Hanahan D, Weinberg RA. Hallmarks of cancer: the next generation. cell. 2011 Mar 4;144(5):646-74.

[**Henneke, 2009**] Henneke M, Diekmann S, Ohlenbusch A, Kaiser J, Engelbrecht V, Kohlschütter A, Krätzner R, Madruga-Garrido M, Mayer M, Opitz L, Rodriguez D. RNASET2-deficient cystic leukoencephalopathy resembles congenital cytomegalovirus brain infection. Nature genetics. 2009 Jul 1;41(7):773.

[**Hildebrandt, 2011**] Hildebrandt JP, Lemke S. Small bite, large impact–saliva and salivary molecules in the medicinal leech, Hirudo medicinalis. Naturwissenschaften. 2011 Dec 1;98(12):995-1008.

[**Hotchkiss, 2003**] Hotchkiss KA, Ashton AW, Klein RS, Lenzi ML, Zhu GH, Schwartz EL. Mechanisms by which tumor cells and monocytes expressing the angiogenic factor thymidine phosphorylase mediate human endothelial cell migration. Cancer research. 2003 Jan 15;63(2):527-33.

[**Huang, 2009**] Huang S. Non-genetic heterogeneity of cells in development: more than just noise. Development. 2009 Dec 1;136(23):3853-62.

[**Huang, 2010**] Huang S. Cell lineage determination in state space: a systems view brings flexibility to dogmatic canonical rules. PLoS Biol. 2010 May 25;8(5):e1000380.

[**Islam, 2000**] Islam MQ, Islam K. A new functional classification of tumor-suppressing genes and its therapeutic implications. Bioessays. 2000 Mar 1;22(3):274-85.

[**Jones, 2003**] Jones D, Kroos N, Anema R, Van Montfort B, Vooys A, Kraats SV, Helm EV, Smits S, Schouten J, Brouwer K, Lagerwerf F. High-level expression of recombinant IgG in the human cell line PER. C6. Biotechnology progress. 2003 Jan 1;19(1):163-8.

[**Klein, 1976**] Klein G. Analysis of malignancy and antigen expression by cell fusion. InFederation proceedings 1976 Aug (Vol. 35, No. 10, pp. 2202-2204).

[**Klein, 2007**] Klein G, Imreh S, Zabarovsky ER. Why do we not all die of cancer at an early age?. Advances in cancer research. 2007 Dec 31;98:1-6.

[**Kleinman, 1986**] Kleinman HK, McGarvey ML, Hassell JR, Star VL, Cannon FB, Laurie GW, Martin GR. Basement membrane complexes with biological activity. Biochemistry. 1986 Jan;25(2):312-8.

[**Klimp, 2001**] Klimp AH, Hollema H, Kempinga C, van der Zee AG, de Vries EG, Daemen T. Expression of cyclooxygenase-2 and inducible nitric oxide synthase in human ovarian tumors and tumor-associated macrophages. Cancer research. 2001 Oct 1;61(19):7305-9.

[**Koide, 1974**] Koide N, Muramatsu T. Endo-β-N-acetylglucosaminidase Acting on Carbohydrate Moieties of Glycoproteins PURIFICATION AND PROPERTIES OF THE ENZYME FROM DIPLOCOCCUS PNEUMONIAE. Journal of Biological Chemistry. 1974 Aug 10;249(15):4897-904.

[**Lemmon, 2010**] Lemmon MA, Schlessinger J. Cell signaling by receptor tyrosine kinases. Cell. 2010 Jun 25;141(7):1117-34.

[**Liang, 2002**] Liang L, Lai Z, Ma W, Zhang Y, Xue Y. AhSL28, a senescence-and phosphate starvation-induced S-like RNase gene in Antirrhinum. Biochimica et Biophysica Acta (BBA)-Gene Structure and Expression. 2002 Nov 13;1579(1):64-71.

[**Locati, 2002**] Locati M, Deuschle U, Massardi ML, Martinez FO, Sironi M, Sozzani S, Bartfai T, Mantovani A. Analysis of the gene expression profile activated by the CC chemokine ligand 5/RANTES and by lipopolysaccharide in human monocytes. The Journal of Immunology. 2002 Apr 1;168(7):3557-62.

[**Lualdi, 2015**] Lualdi M, Pedrini E, Rea K, Monti L, Scaldaferri D, Gariboldi M, Camporeale A, Ghia P, Monti E, Tomassetti A, Acquati F, Taramelli R. Pleiotropic modes of action in tumor cells of RNASET2, an evolutionary highly conserved extracellular RNase. Oncotarget. 2015 Apr 10;6(10):7851.

[**Luhtala, 2010**] Luhtala N, Parker R. T2 Family ribonucleases: ancient enzymes with diverse roles. Trends in biochemical sciences. 2010 May 31;35(5):253-9.

[**Maeß, 2014**] Maeß MB, Wittig B, Cignarella A, Lorkowski S. Reduced PMA enhances the responsiveness of transfected THP-1 macrophages to polarizing stimuli. Journal of immunological methods. 2014 Jan 15;402(1):76-81.

[**Mantovani, 2002**] Mantovani A, Sozzani S, Locati M, Allavena P, Sica A. Macrophage polarization: tumor-associated macrophages as a paradigm for polarized M2 mononuclear phagocytes. Trends in immunology. 2002 Nov 1;23(11):549-55.

[**Mantovani, 2004**] Mantovani A, Allavena P, Sica A. Tumour-associated macrophages as a prototypic type II polarised phagocyte population: role in tumour progression. European Journal of Cancer. 2004 Jul 31;40(11):1660-7.

[**Mantovani, 2005**] Mantovani A, Sica A, Locati M. Macrophage polarization comes of age. Immunity. 2005 Oct 31;23(4):344-6.

[**Martinez, 2006**] Martinez FO, Gordon S, Locati M, Mantovani A. Transcriptional profiling of the human monocyte-to-macrophage differentiation and polarization: new molecules and patterns of gene expression. The Journal of Immunology. 2006 Nov 15;177(10):7303-11.

[**Martinez, 2014**] Martinez FO, Gordon S. The M1 and M2 paradigm of macrophage activation: time for reassessment. F1000Prime Rep. 2014 Mar 3;6(13.10):12703.

[**Matsushima, 1999**] Matsushima K, Larsen CG, DuBois GC, Oppenheim JJ. Purification and characterization of a novel monocyte chemotactic and activating factor produced by a human myelomonocytic cell line. J Exp Med. 1989 Apr 1;169(4):1485-90.

[**McClure, 1990**] McClure BA, Gray JE, Anderson MA, Clarke AE. Self-incompatibility in Nicotiana alata involves degradation of pollen rRNA. Nature. 1990 Oct 25;347(6295):757-60.

[**Medina, 2011**] Medina RJ, O'Neill CL, Michelle O'Doherty T, Knott H, Guduric-Fuchs J, Gardiner TA, Stitt AW. Myeloid angiogenic cells act as alternative M2 macrophages and modulate angiogenesis through interleukin-8. Molecular medicine. 2011 Sep 1;17(9):1045.

[**Mills, 2000**] Mills CD, Kincaid K, Alt JM, Heilman MJ, Hill AM. M-1/M-2 macrophages and the Th1/Th2 paradigm. The Journal of Immunology. 2000 Jun 15;164(12):6166-73.

[**Mosser, 2008**] Mosser DM, Edwards JP. Exploring the full spectrum of macrophage activation. Nature reviews immunology. 2008 Dec 1;8(12):958-69.

[**Murray, 2014**] Murray PJ, Allen JE, Biswas SK, Fisher EA, Gilroy DW, Goerdt S, Gordon S, Hamilton JA, Ivashkiv LB, Lawrence T, Locati M. Macrophage activation and polarization: nomenclature and experimental guidelines. Immunity. 2014 Jul 17;41(1):14-20.

[**Nakayama, 2007**] Nakayama K, Nakayama N, Jinawath N, Salani R, Kurman RJ, Shih IM, Wang TL. Amplicon profiles in ovarian serous carcinomas. International journal of cancer. 2007 Jun 15;120(12):2613-7.

[**Nathan, 1983**] Nathan CF, Murray HW, Wiebe ME, Rubin BY. Identification of interferon-γ as the lymphokine that activates human macrophage oxidative metabolism and antimicrobial activity. J. exp. Med. 1983;158(670):l983.

[**Nokhandani, 2015**] Nokhandani AM, Otaghsara SM, Abolfazli MK, Karimi M, Adel F, Babapour H, Atae G. A review of new method of cold plasma in cancer treatment. Scholars Acad. J. Biosci. 2015;3:222-30.

[**Nowell, 1976**] Nowell PC. The clonal evolution of tumor cell populations. Science. 1976 Oct 1;194(4260):23-8.

[**Orphanos, 1995**] Orphanos V, McGown G, Hey Y, Thorncroft M, Santibanez-Koref M, Russell SE, Hickey I, Atkinson RJ, Boyle JM. Allelic imbalance of chromosome 6q in ovarian tumours. British journal of cancer. 1995 Apr;71(4):666.

[**Park, 2007**] Park EK, Jung HS, Yang HI, Yoo MC, Kim C, Kim KS. Optimized THP-1 differentiation is required for the detection of responses to weak stimuli. Inflammation research. 2007 Jan 14;56(1):45-50.

[**Pollard, 2008**] Pollard JW. Macrophages define the invasive microenvironment in breast cancer. Journal of leukocyte biology. 2008 Sep 1;84(3):623-30.

[**Rollins, 1999**] Rollins B. Chemokines and Cancer. Totowa, NJ: Humana Press; 1999.

[**Saito, 1992**] Saito S, Saito H, Koi S, Sagae S, Kudo R, Saito J, Noda K, Nakamura Y. Fine-scale deletion mapping of the distal long arm of chromosome 6 in 70 human ovarian cancers. Cancer research. 1992 Oct 15;52(20):5815-7.

[**Satoh, 2003**] Satoh T, Saika T, Ebara S, Kusaka N, Timme TL, Yang G, Wang J, Mouraviev V, Cao G, Thompson TC. Macrophages transduced with an adenoviral vector expressing interleukin 12 suppress tumor growth and metastasis in a preclinical metastatic prostate cancer model. Cancer research. 2003 Nov 15;63(22):7853-60.

[**Schikorski, 2008**] Schikorski D, Cuvillier-Hot V, Leippe M, Boidin-Wichlacz C, Slomianny C, Macagno E, Salzet M, Tasiemski A. Microbial challenge promotes the regenerative process of the injured central nervous system of the medicinal leech by inducing the synthesis of antimicrobial peptides in neurons and microglia. The Journal of Immunology. 2008 Jul 15;181(2):1083-95.

[**Schnell, 1999**] Schnell SA, Staines WA, Wessendorf MW. Reduction of lipofuscin-like autofluorescence in fluorescently labeled tissue. Journal of Histochemistry & Cytochemistry. 1999 Jun;47(6):719-30.

[**Schoppmann, 2002**] Schoppmann SF, Birner P, Stöckl J, Kalt R, Ullrich R, Caucig C, Kriehuber E, Nagy K, Alitalo K, Kerjaschki D. Tumor-associated macrophages express lymphatic endothelial growth factors and are related to peritumoral lymphangiogenesis. The American journal of pathology. 2002 Sep 30;161(3):947-56.

[**Schorn, 2015a**] Schorn T, Drago F, De Eguileor M, Valvassori R, Vizioli J, Tettamanti G, Grimaldi A. AIF-1. Invert Survival J. 201512:129–141.

[**Schorn, 2015b**] Schorn T, Drago F, Tettamanti G, Valvassori R, de Eguileor M, Vizioli J, Grimaldi A. Homolog of allograft inflammatory factor-1 induces macrophage migration during innate immune response in leech. Cell and tissue research. 2015 Mar 1;359(3):853-64.

[**Schwartz, 2007**] Schwartz B, Shoseyov O, Melnikova VO, McCarty M, Leslie M, Roiz L, Smirnoff P, Hu GF, Lev D, Bar-Eli M. ACTIBIND, a T2 RNase, competes with angiogenin and inhibits human melanoma growth, angiogenesis, and metastasis. Cancer research. 2007 Jun 1;67(11):5258-66.

[**Shay, 2000**] Shay JW, Wright WE. Hayflick, his limit, and cellular ageing. Nature reviews Molecular cell biology. 2000 Oct 1;1(1):72-6.

[**Sherr, 2002**] Sherr CJ, McCormick F. The RB and p53 pathways in cancer. Cancer cell. 2002 Aug 31;2(2):103-12.

[**Smirnoff, 2006**] Smirnoff P, Roiz L, Angelkovitch B, Schwartz B, Shoseyov O. A recombinant human RNASET2 glycoprotein with antitumorigenic and antiangiogenic characteristics. Cancer. 2006 Dec 15;107(12):2760-9.

[**Simon, 2013**] Simon R. Drug-diagnostics co-development in oncology.

[**Sonnenschein, 2000**] Sonnenschein C, Soto AM. Somatic mutation theory of carcinogenesis: why it should be dropped and replaced. Molecular carcinogenesis. 2000 Dec 1;29(4):205-11.

[**Stein, 1992**] Stein M, Keshav S, Harris N, Gordon S. Interleukin 4 potently enhances murine macrophage mannose receptor activity: a marker of alternative immunologic macrophage activation. Journal of Experimental Medicine. 1992 Jul 1;176(1):287-92.

[**Steinfelder, 2009**] Steinfelder S, Andersen JF, Cannons JL, Feng CG, Joshi M, Dwyer D, Caspar P, Schwartzberg PL, Sher A, Jankovic D. The major component in schistosome eggs responsible for conditioning dendritic cells for Th2 polarization is a T2 ribonuclease (omega-1). Journal of Experimental Medicine. 2009 Aug 3;206(8):1681-90.

[**Stout, 2004**] Stout RD, Suttles J. Functional plasticity of macrophages: reversible adaptation to changing microenvironments. Journal of leukocyte biology. 2004 Sep 1;76(3):509-13.

[**Suehiro, 2000**] Suehiro Y, Sakamoto M, Umayahara K, Iwabuchi H, Sakamoto H, Tanaka N, Takeshima N, Yamauchi K, Hasumi K, Akiya T, Sakunaga H. Genetic aberrations detected by comparative genomic hybridization in ovarian clear cell adenocarcinomas. Oncology. 2000 Jun 30;59(1):50-6.

[**Talmadge, 2010**] Talmadge JE, Fidler IJ. AACR centennial series: the biology of cancer metastasis: historical perspective. Cancer research. 2010 Jul 15;70(14):5649-69.

[**Tapper, 1997**] Tapper J, BÃ¼tzow R, WahlstrÃ T. Evidence for divergence of DNA copy number changes in serous, mucinous and endometrioid ovarian carcinomas. British journal of cancer. 1997;75(12):1782.

[**Tettamanti, 2004**] Tettamanti G, Grimaldi A, Rinaldi L, Arnaboldi F, Congiu T, Valvassori R, Eguileor M. The multifunctional role of fibroblasts during wound healing in Hirudo medicinalis (Annelida, Hirudinea). Biology of the Cell. 2004 Aug 1;96(6):443-55.

[**Tettamanti, 2005**] Tettamanti G, Grimaldi A, Rinaldi L, Arnaboldi F, Congiu T, Valvassori R, Eguileor M. The multifunctional role of fibroblasts during wound healing in Hirudo medicinalis (Annelida, Hirudinea). Biology of the Cell. 2004 Aug 1;96(6):443-55.

[**Thompson, 2009**] Thompson DM, Parker R. The RNase Rny1p cleaves tRNAs and promotes cell death during oxidative stress in Saccharomyces cerevisiae. The Journal of cell biology. 2009 Apr 6;185(1):43-50.

[**Tibiletti, 1996**] Tibiletti MG, Bernasconi B, Furlan D, Riva C, Trubia M, Buraggi G, Franchi M, Bolis P, Mariani A, Frigerio L, Capella C. Early involvement of 6q in surface epithelial ovarian tumors. Cancer research. 1996 Oct 1;56(19):4493-8.

[**Tibiletti, 1998**] Tibiletti MG, Trubia M, Ponti E, Sessa L, Acquati F, Furlan D, Bernasconi B, Fichera M, Mihalich A, Ziegler A, Volz A. Physical map of the D6S149-D6S193 region on chromosome 6Q27 and its involement in benign surface epithelial ovarian tumours. Oncogene. 1998 Apr;16(12):1639-42.

[**Tirosh, 2016**] Tirosh I, Izar B, Prakadan SM, Wadsworth MH, Treacy D, Trombetta JJ, Rotem A, Rodman C, Lian C, Murphy G, Fallahi-Sichani M. Dissecting the multicellular ecosystem of metastatic melanoma by single-cell RNA-seq. Science. 2016 Apr 8;352(6282):189-96.

[**Tschopp, 1987**] Tschopp JF, Sverlow G, Kosson R, Craig W, Grinna L. High-level secretion of glycosylated invertase in the methylotrophic yeast, Pichia pastoris. Nature Biotechnology. 1987 Dec 1;5(12):1305-8.

[**Vidalino, 2012**] Vidalino L, Monti L, Haase A, Moro A, Acquati F, Taramelli R, Macchi P. Intracellular trafficking of RNASET2, a novel component of P-bodies. Biology of the Cell. 2012 Jan 1;104(1):13-21.

[**Wang, 2017**] Wang Y, Lin YX, Qiao SL, An HW, Ma Y, Qiao ZY, Rajapaksha RY, Wang H. Polymeric nanoparticles promote macrophage reversal from M2 to M1 phenotypes in the tumor microenvironment. Biomaterials. 2017 Jan 31;112:153-63.

[**Würden, 1993**] Würden S, Homberg U. A simple method for immunofluorescent double staining with primary antisera from the same species. Journal of Histochemistry & Cytochemistry. 1993 Apr 1;41(4):627-30.

[**Zhou, 2016**] Zhou JX, Isik Z, Xiao C, Rubin I, Kauffman SA, Schroeder M, Huang S. Systematic drug perturbations on cancer cells reveal diverse exit paths from proliferative state. Oncotarget. 2016 Feb 16;7(7):7415.

PUBLICATIONS

Baranzini N, Pedrini E, Girardello R, Tettamanti G, de Eguileor M, Taramelli R, Acquati F, Grimaldi A. Human recombinant RNASET2-induced inflammatory response and connective tissue remodeling in the medicinal leech. Cell and Tissue Research. 2017 Jan 9:1-5.

Turconi, G., Scaldaferri, D., Fabbri, M., Monti, L., Lualdi, M., Pedrini, E., Gribaldo, L., Taramelli, R., Acquati, F."RNASET2 silencing affects miRNAs and target gene expression pattern in a human ovarian cancer cell model". International Journal of Oncology 49.6 (2016): 2637-2646.

Lualdi M*, Pedrini E*, Petroni F, Näsman J, Lindqvist C, Scaldaferri D, Taramelli R, Inforzato A, Acquati F. New Strategies for Expression and Purification of Recombinant Human RNASET2 Protein in Pichia pastoris. Mol Biotechnol. 2015 Jun;57(6):513-25. *Equal contribtion.

Lualdi M, Pedrini E, Rea K, Monti L, Scaldaferri D, Gariboldi M, Camporeale A, Ghia P, Monti E, Tomassetti A, Acquati F, Taramelli R. Pleiotropic modes of action in tumor cells of RNASET2, an evolutionary highly conserved extracellular RNase. Oncotarget. 2015 Apr 10;6(10):7851-65.